REVIEW

Check for updates

AIEgens for synergistic anticancer therapy

Xinyan Lyu, †[a] Junjie Yu,†[a] Liping Zhang,†[a] Yun Zhao,[a] Zijie Qiu,[a] Youbai Chen,*[c] Zheng Zhao *[ab] and Ben Zhong Tang*[ad]

Cancer is a mortal disease that can invade other parts of the body and cause severe complications. Despite their continuous progress, conventional cancer therapies including surgery, chemotherapy, and radiation therapy have their inherent limitations. To improve the precision of cancer treatment, maximize the therapeutic effect and minimize mortality, synergistic therapies combining imaging guiding technologies, phototherapy, and other therapies have emerged due to the mutually strengthening therapeutic efficacy. However, traditional organic phototherapeutic agents are limited since their aggregation in aqueous media usually affects both their luminescence behavior and therapeutic effect. In contrast, aggregate-induced emission luminogens (AIEgens) provide an ideal solution to develop phototherapy with bright fluorescence and a significant treatment effect in the aggregate state. Combining AIE-based phototherapy and conventional therapies benefits from synergistic effects and extends the potential of developing accurate cancer therapy. AIE-based synergistic therapy has been popularly discussed with such unexplored potential in recent years. This review will introduce the most recent progress of AIE-based synergistic cancer therapy.

[a] *The Second Affiliated Hospital, School of Medicine, School of Science and Engineering, Shenzhen Institute of Aggregate Science and Technology, The Chinese University of Hong Kong, Shenzhen, Guangdong 518172, China. E-mail: zhaozheng@cuhk.edu.cn, tangbenz@cuhk.edu.cn*

[b] *HKUST Shenzhen Research Institute, Shenzhen 518057, China*

[c] *Department of Plastic and Reconstructive Surgery, The First Medical Center of Chinese PLA General Hospital, 28 Fuxing Rd, Beijing, 100853, China. E-mail: chenyoubai@301hospital.com.cn*

[d] *Department of Chemistry, Hong Kong Branch of Chinese National Engineering Research Center for Tissue Restoration and Reconstruction, The Hong Kong University of Science and Technology, 100071 Hong Kong, China*

† These authors contributed equally to this work.

1. Introduction

Cancer, one of the leading causes of death globally, is relatively challenging to cure due to its uncontrollable cell proliferation properties.[1–3] Conventional therapeutic methods, including surgical treatment, chemotherapy, and radiation therapy, are the primary cancer therapies in clinics, although more advanced therapeutic modes like gene therapy and immunotherapy have been widely investigated and explored recently. However, these therapies generally have various drawbacks, including drug resistance, severe side effects, limited application scenarios, and potential gene mutation.[4–7] Compared with

Xinyan Lyu is an undergraduate student at the School of Science and Engineering, the Chinese University of Hong Kong, Shenzhen. She currently majors in Chemical Science. Her current research focuses on luminescent functional materials and mechanisms of aggregation-induced emission.

Xinyan Lyu

Junjie Yu is an undergraduate student in the Chinese University of Hong Kong, Shenzhen. His major is Chemistry Science. His research interest includes the design and synthesis of functional organic AIE luminescent molecules.

Junjie Yu

This journal is © The Royal Society of Chemistry 2023

J. Mater. Chem. B, 2023, **11**, 5953–5975 | **5953**

conventional therapies, phototherapy exhibits great potential for treating various types of cancers with a lot of advantages, *i.e.*, non-invasiveness, no tolerance, low side-effects, convenient operation, *etc.*[8] Typical phototherapy modes like photothermal therapy (PTT) that can convert light energy into heat to ablate tumors, and photodynamic therapy (PDT) that produces reactive oxygen species (ROS) to exert cytotoxic activity in cancer cells have attracted great attention.[9–11] More importantly, apart from the therapeutic effect, many phototherapeutic agents also exhibit fluorescence imaging properties, enabling the integration of diagnostic and therapeutic functions into one platform to achieve accurate image-guided cancer treatment.[12]

Although phototherapy is considered a safe and secure approach to destroying tumor cells, the therapeutic efficiency of PTT or PDT alone is still unsatisfactory. In this regard, integrating phototherapy and other therapeutic modalities has great potential in precise diagnostics and more efficient

therapy.[13–16] These synergistic therapies combining more than one therapeutic modality are anticipated to develop new treatments to meet the requirements of future personalized therapeutic approaches.[17] In addition, in comparison with inorganic fluorophores, organic fluorophores demonstrate excellent biocompatibility and good modifiability, consequently having more potential for clinical application.[18–20]

Nevertheless, conventional organic fluorophores such as rhodamine, fluorescein, and cyanine derivatives have one fatal limitation of the aggregation-caused quenching (ACQ) effect.[21–23] In the aggregate state, most of them suffer from severe self-quenching and a poor signal-to-noise ratio, resulting in a poor imaging performance. Furthermore, the PDT effect of many traditional photosensitizers would be reduced due to the aggregation boosted non-radiative decay.[24,25] In contrast, aggregation-induced emission (AIE) fluorophores provide an elegant alternative to construct synergistic theranostics due to

Liping Zhang

Liping Zhang received her PhD degree in chemical technology from Sichuan University. She is currently conducting her postdoctoral research in Prof. Ben Zhong Tang's group at the School of Science and Engineering, the Chinese University of Hong Kong, Shenzhen. Her current research interests mainly focus on stimuli-responsive AIE materials and exploration of their biomedical applications.

Yun Zhao

Yun Zhao received his BE degree in Organic Chemistry and Chemical Engineering from Zhejiang University of Technology (2014). After several years scientific research training at Tsinghua University, he studied at The Chinese University of Hong Kong, Shenzhen under the supervision of Prof. Zheng Zhao and Prof. Ben Zhong Tang.
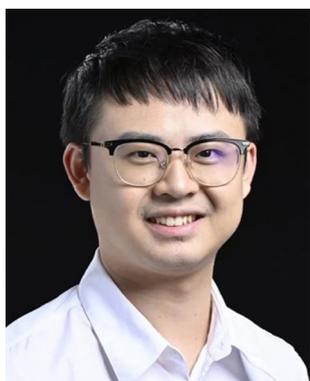
Zijie Qiu

Zijie Qiu received his bachelor's degree in chemistry from Fudan University in 2014 and PhD in chemistry at the Hong Kong University of Science and Technology in 2018 under the supervision of Prof. Ben Zhong Tang. After graduation, he joined the group of Prof. Dr Klaus Müllen at the Max Planck Institute for Polymer Research (MPIP) for postdoctoral research as a Alexander von Humboldt Fellow and was later promoted to Group Leader in April 2020. He is currently working as a tenure-track Assistant Professor and Presidential Young Scholar at the Chinese University of Hong Kong, Shenzhen. His research interests include the syntheses and applications of organic luminescent molecules and polymers with a special focus on chirality.

Youbai Chen

Youbai Chen is an associate professor at the Chinese PLA General Hospital. He received his MD/PhD from Chinese PLA Medical School and University of Texas MD Anderson Cancer Center in 2016 and his MMS from Harvard Medical School in 2019. He conducted his fellowship at Massachusetts General Hospital from 2017 to 2019. He joined the Department of Plastic and Reconstructive Surgery Chinese PLA General Hospital and has worked as a surgeon and researcher since 2013. Clinically, he specialized in reconstruction of craniomaxillofacial trauma, deformity, and defect. His current research focuses on fluorescence-guided treatment for advanced skin and soft tissue tumors using multifunctional materials.

5954 | *J. Mater. Chem. B*, 2023, **11**, 5953–5975

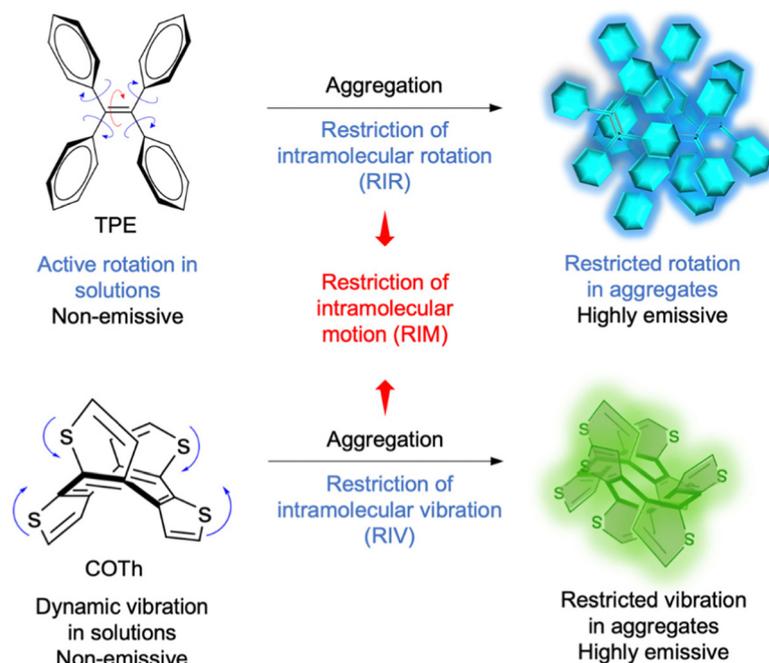This journal is © The Royal Society of Chemistry 2023

Fig. 1 The proposed mechanism of AIE phenomena observed in organic molecules. Tetraphenylethene (TPE) is non-emissive in solution but becomes emissive in the aggregate state due to RIR. Cyclooctatetrathiophene (COTh) presents similar AIE properties due to RIV. Reproduced with permission from Wiley-VCH, copyright 2020.[25]

their outstanding advantages of high emission intensity in the aggregation state, large Stokes shift, remarkable photostability, as well as *in vivo* switch-on ability.[26] The AIE mechanism, restriction of intramolecular motion (RIM), as shown in Fig. 1, can be categorized as a restriction of intramolecular rotation (RIR) and restriction of intramolecular vibration (RIV), which can boost non-radiative decay of isolated molecules to show weak emission and block non-radiative decay of aggregate-state molecules to enhance emission.[25,27] Moreover, their therapeutic effect such as PDT performance could even be

enhanced in aggregates which provides more possibility for developing advanced synergistic theranostics.

To date, numerous AIE-based phototherapies have been developed for tumor treatments, including a large amount of synergistic therapeutic systems. However, there has been no comprehensive survey of AIEgen-based synergistic systems.[28] This review thus summarizes the latest progress of synergistic anticancer therapy based on AIEgens (Scheme 1). The contents discussed under this topic mainly include photo-chemotherapy, photo-immunotherapy, and photo-radiation

Zheng Zhao is an assistant professor at the Chinese University of Hong Kong, Shenzhen. He received his PhD from Shanghai Institute of Organic Chemistry, Chinese Academy of Science in 2014. He conducted his postdoctoral research at the Hong Kong University of Science and Technology from 2015 to 2019. In 2020, he joined the School of Chemistry and Chemical Engineerin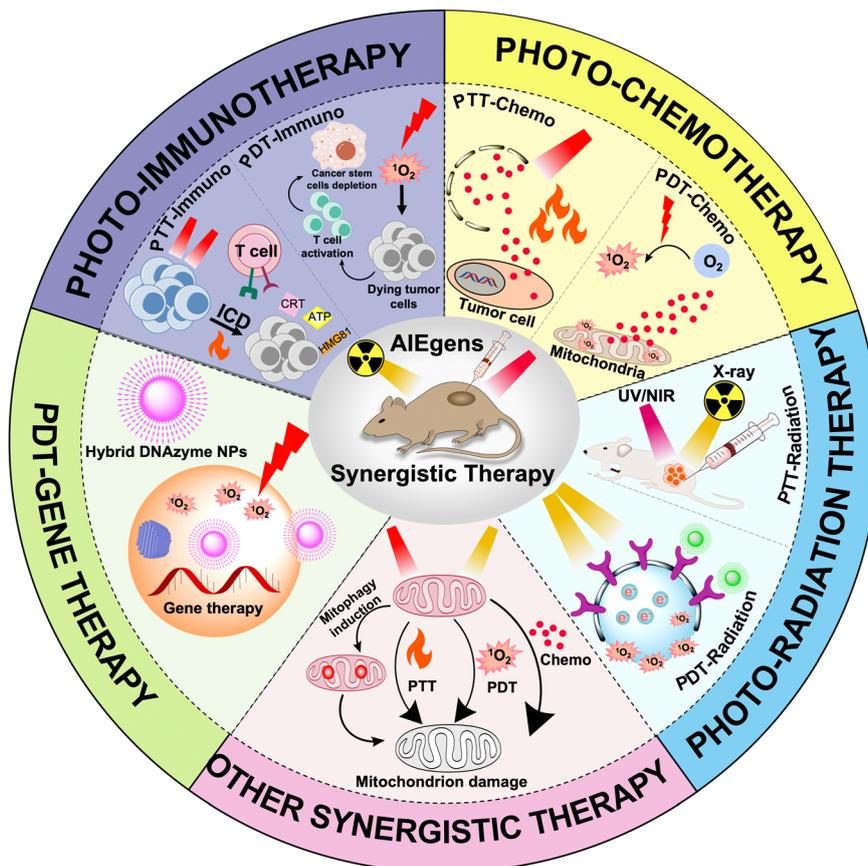g at Southeast University. In 2021, he moved to The Chinese University of Hong Kong, Shenzhen and worked as an assistant professor and a Presidential Young Scholar. His current research focuses on luminescent functional materials and their bioapplications.

Zheng Zhao

Ben Zhong Tang is a Distinguished Presidential Chair Professor at the school of science and engineering, the Chinese University of Hong Kong, Shenzhen. He received his PhD from Kyoto University in 1988. He conducted his postdoctoral research at the University of Toronto from 1989 to 1994. He joined HKUST in 1994 and was promoted to chair professor in 2008 and Stephen K. C. Cheong Professor of Science in 2013. He was elected to the Chinese Academy of Sciences in 2009. Currently, he works as a Distinguished Presidential Chair Professor at The Chinese University of Hong Kong, Shenzhen. His research interests include the exploration of new advanced materials, new luminescent processes, and polymer chemistry.

Ben Zhong Tang

This journal is © The Royal Society of Chemistry 2023

J. Mater. Chem. B, 2023, **11**, 5953–5975 | **5955**

Scheme 1 AIEgen-based synergistic therapy.

therapy *etc.*, in which more detailed classification like PDT-chemotherapy, PTT-chemotherapy, PDT-immunotherapy, PTT-immunotherapy, PDT-radiation therapy, PDT-gene therapy *etc.* will be presented and discussed. We hope this review can provide an overview of AIE-based synergistic therapies and stimulate more interest in this area.

2. Photo-chemotherapy

Chemotherapy uses chemical drugs to disrupt the functions of tumor cells, reduce tumor growth, and induce the death of tumor cells, contributing to the therapeutic effects of cancer.[29] However, chemotherapy drugs can also damage normal cells while killing tumor cells, resulting in severe drug resistance and some side effects.[30] Photo-chemo therapy uses phototherapy like PDT or PTT to synergize with chemotherapy to improve the therapeutic effect, removing the limitations of using chemotherapy alone.[31,32]

2.1. PTT-chemotherapy

PTT is a noninvasive and low-toxic approach to killing tumors.[33] The photothermal agents absorb light at a specific wavelength, convert light energy into heat to thermally ablate tumor cells, and elevate the tissue temperature. The resulting overheating microenvironment of the tissue can enhance cell membrane permeability and improve the cellular uptake of the drugs, increasing the sensitivity of chemotherapy.[34,35]

In 2016, Wei *et al.* developed a novel AIEgen-based nanosystem *via* paclitaxel (PTX) induced protein assembly for the first time, which achieved fluorescence imaging-guided synergistic PTT-chemotherapy *in vivo*.[36] The AIEgen PhENH$_2$ was conjugated with human serum albumin (HSA), a major component of serum proteins contributing to inherent biocompatibility, for fluorescent imaging reagent, while cyclic arginine–glycine–aspartic acid (cRGD) was used to premodify HSA as the targeting moiety. Polypyrrole (PPy) acted as a PTT agent to increase the tumor temperature for tumor ablation, and PTX was assembled to form a HSA-PhENH$_2$-PPy-PTX-cRGD nanoplatform (Fig. 2a). Since the targeting agent cRGD could bind specifically to αvβ3-integrin, U87MG human primary glioblastoma cells overexpressing αvβ3-integrin were chosen for the cell experiment (Fig. 2b). With intravenous injection of HSA-PhENH$_2$-PPy-PTX-cRGD into tumor-bearing mice and exposure to an 808 nm laser, the average temperature of the tumor region in mice increased rapidly, which indicated the constructed nanoplatform was feasible for PTT (Fig. 2c). Furthermore, the tumor growth of mice with HSA-PhENH$_2$-PPy-PTX-cRGD was inhibited effectively (Fig. 2d), proving the efficacy of tumor-targeted synergistic PTT-chemo nanotheranostics based on AIEgens.
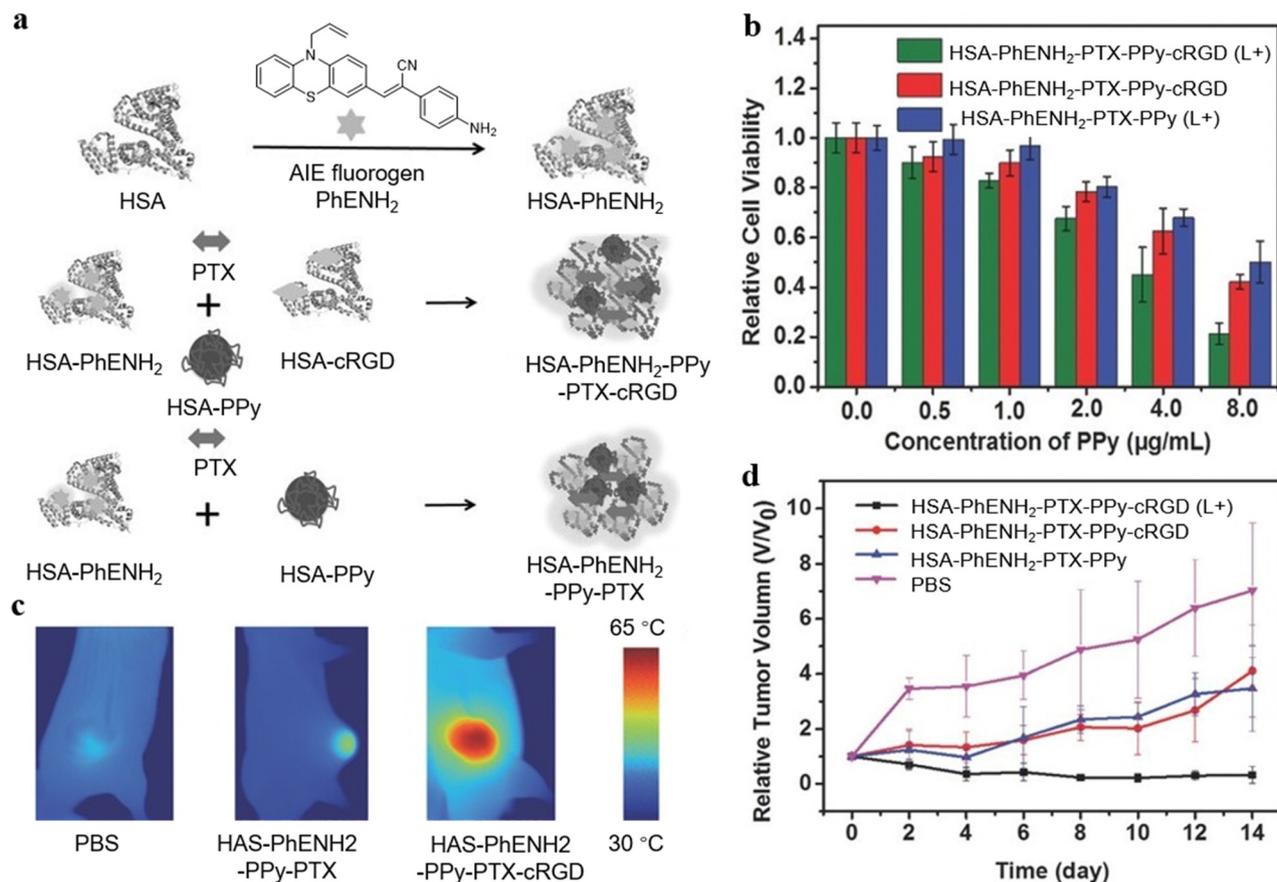
5956 | *J. Mater. Chem. B*, 2023, **11**, 5953–5975

This journal is © The Royal Society of Chemistry 2023

Fig. 2 (a) Illustration of the preparation of HAS-PhENH$_2$ and the PTX induced assembly of AIEgens. (b) Relative cell viability of U87MG cells after incubation of HSA-PhENH$_2$-PPy-PTX-cRGD and HSA-PhENH$_2$-PPy-PTX with or without 808 nm laser irradiation. The cells were washed with phosphate buffer solution (PBS) and then incubated in fresh medium for 24 h before the CCK-8 assay. (c) IR thermal images of mice bearing U87MG tumors treated with PBS, HSA-PhENH$_2$-PPy-PTX, and HSA-PhENH$_2$-PPy-PTX-cRGD after exposure to 808 nm laser irradiation for 5 min. (d) The relative tumor growth curves of different groups of tumor–bearing mice after different treatments. Reproduced with permission from Wiley-VCH, copyright 2016.[36]

An, Yu, and Zhang *et al.* developed a synergistic PTT-chemotherapy nanoplatform based on IR-797 chloride (Fig. 3a).[37] IR-797 as a AIEgen and PTT agent was self-assembled into the polymer to form PEG-IR-797 NPs and could work as a chemotherapeutic drug to kill tumor cells (Fig. 3b). The PEG-IR-797 NP could achieve real-time monitoring of cancer treatment by its fluorescence imaging (Fig. 3c). Moreover, the PEG-IR-797 NP under light irradiation could not only trigger chemotherapy but also induce PTT to accomplish synergistic PTT-chemotherapy (Fig. 3d).

Recently, NIR fluorescence of AIEgens has attracted great attention due to its noninvasiveness, high sensitivity, and precise tumor visualization abilities. Combining NIR fluorescence with a photothermal process could effectively enhance the cellular uptake of drugs due to increasing permeability of the cell membrane and accelerating drug delivery.[38–41] Zhang, Wang, Hou, and Tang *et al.* constructed multifunctional BITT@BSA-DSP NPs with photo-enhanced chemotherapeutic effects (Fig. 4a).[42] Glutathione (GSH) was utilized to improve chemotherapy efficiency. As shown in Fig. 4b, the antitumor drug release behavior of cisplatin Pt was investigated: the

release percentage of Pt with GSH only was 39.4% at 3 h, while the release percentage of Pt with GSH under light irradiation reached 71.2% at 3 h, demonstrating the photothermal effects generated by BITT AIEgens could effectively enhance disaggregation of the NPs and facilitate drug release to improve chemotherapeutic efficacy. Moreover, compared with PBS, BITT@BSA NPs and BITT@BSA-DSP NPs could increase temperature quickly in the tumor region to perform PTT (Fig. 4c). Therefore, the photoactive agents with AIE properties and anticancer drug could lower the dosage of chemotherapeutic drug, thus diminishing side-effects created by the drug.

2.2. PDT-chemotherapy

Many PSs have been developed, which can be categorized into two types with different mechanisms when considering the type of ROS. The type I reaction involves photo-induced electron transfer and is characterized by hypoxia-tolerance; while the type II reaction involves energy transfer to oxygen and produces singlet oxygen species ($^1O_2$).[43,44] Combining PDT and chemotherapy can effectively address limitations of drug resistance and the side effects of chemotherapy, resulting in a "1 + 1 > 2"
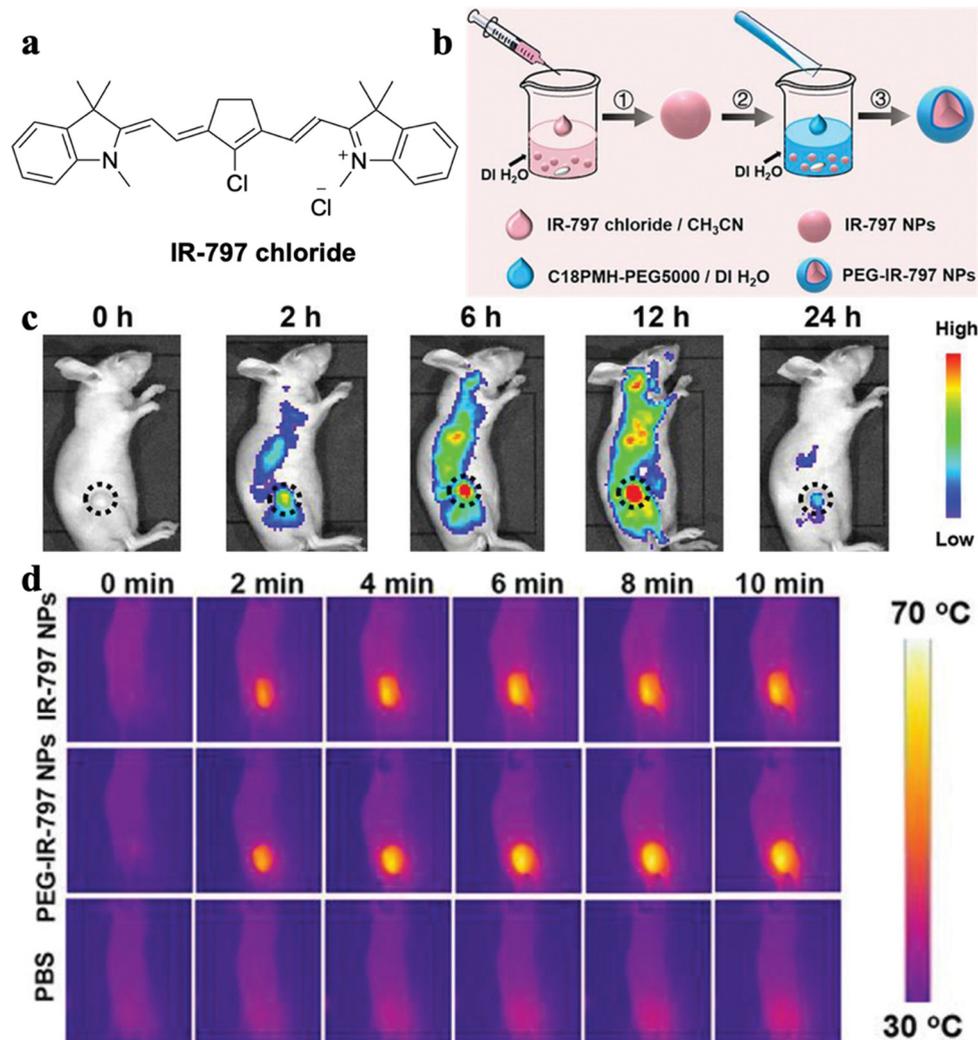
This journal is © The Royal Society of Chemistry 2023

J. Mater. Chem. B, 2023, **11**, 5953–5975 | **5957**

Fig. 3 (a) Molecular structure of IR-797 chloride. (b) Schematic illustration of the preparation process of PEG-IR-797 NPs. (c) *In vivo* fluorescence imaging of HeLa tumor-bearing mice after i.v. injection of PEG-IR-797 NPs with different time periods. (d) *In vivo* IR thermal imaging of HeLa tumor-bearing mice with different treatments under 808 laser irradiation. Reproduced with permission from Wiley-VCH, copyright 2019.[37]

synergistic effect. Yan *et al.* replaced one amine ligand of Pt with a nitrogenous AIE-based PS (BT), thus achieving a high-efficiency antitumor drug (BT-Pt).[45] BT-Pt exhibits NIR fluorescence with a large Stokes shift, which could guide the location of the drug (Fig. 5a and b). The confocal laser scanning microscopy (CLSM) images indicated effective cellular uptake of BT-Pt in HeLa cells as an obvious fluorescence signal was observed from the cytoplasm (Fig. 5c). More significantly, compared to BT, the ROS generation efficiency of BT-Pt has been highly promoted by the fabrication of Pt. Consequently, BT-Pt exhibited favorable therapeutic efficacy for HeLa cells under light irradiation, which was attributed to its synergetic effect of PDT-chemotherapy (Fig. 5d). The design strategy of such platinated PSs showed great potential in developing multifunctional anticancer drugs with combinatorial PDT-chemotherapy.

To avoid the side effect of the PSs to normal tissues, researchers have developed specific tumor microenvironment-activated PSs to silence the photosensitivity of PSs in normal tissue locations. After entering cancer cells, the PS-loaded probes disassemble under reaction with a specific substance, and the fluorescence property and the photosensitivity of PSs are restored. Gao, Ren, and Tang *et al.* developed a dual-organelle-targeted probe for precise synergistic PDT-chemotherapy.[46] The probe could decompose in the acidic lysosome and then release the mitochondria-targeted chemotherapeutic agent AIE-Mito-TPP and commercial PSs AlPcSNa$_4$ (Fig. 6a). The fluorescence of the two agents is activated simultaneously for *in situ* monitoring of the decomposition process of the nanoparticles. The AIE-Mito-TPP could significantly disrupt the mitochondria by decreasing the membrane potential and restraining ATP synthesis, and the AlPcSNa$_4$ could generate ROS and break lysosomes. The experiment results showed that the probe exhibited strong cytotoxicity towards melanoma A375 cells, and the *in vivo* tumor growth could be significantly restrained (Fig. 6b and c). These

5958 | *J. Mater. Chem. B*, 2023, **11**, 5953–5975
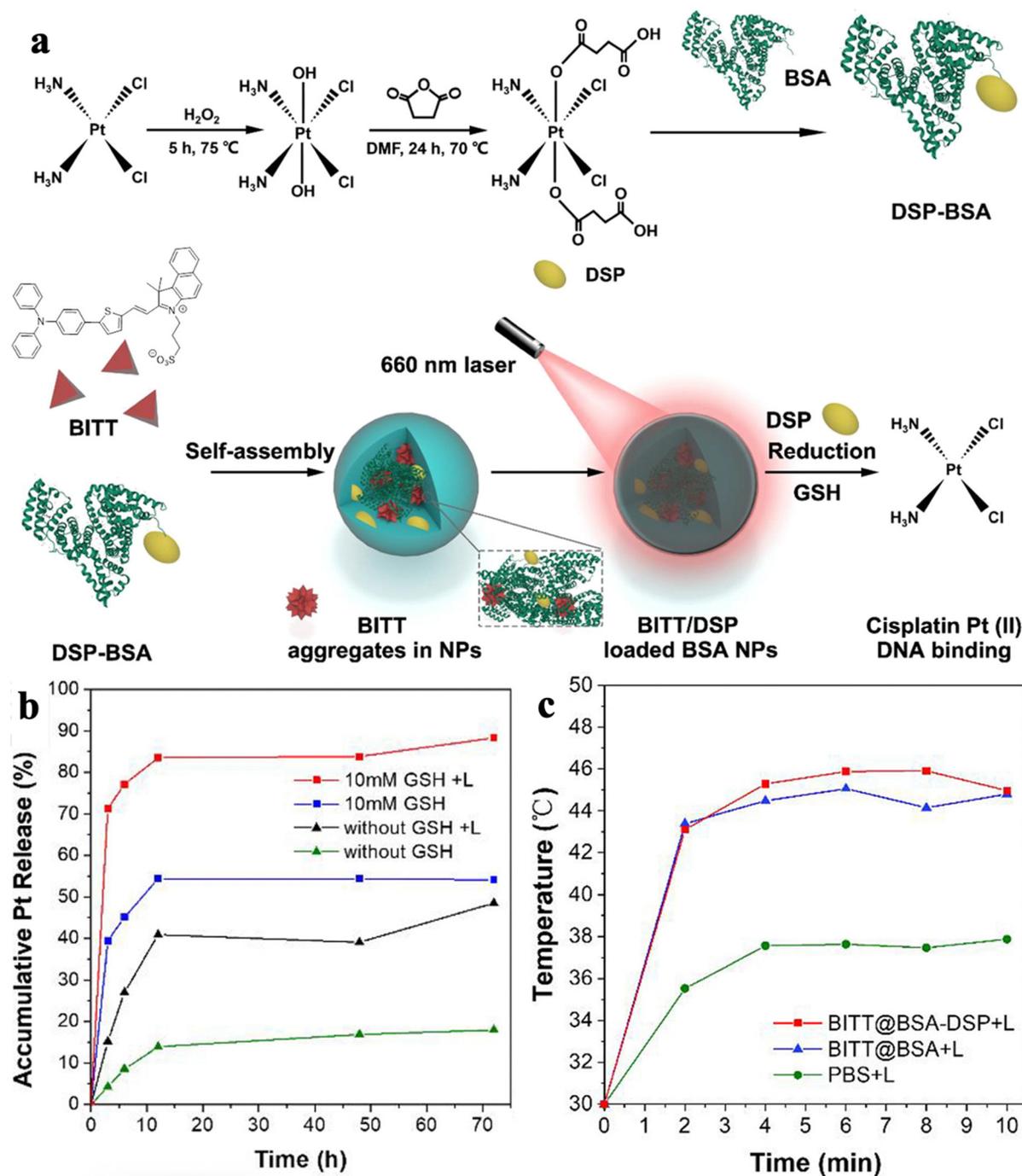
This journal is © The Royal Society of Chemistry 2023

Fig. 4 (a) Schematic illustration of the preparation process of BITT@BSA-DSP NPs. (b) The accumulative Pt release under different conditions. (c) Average temperature of MB49 tumor regions in the mice with different treatments. Reproduced with permission from American Chemical Society, copyright 2022.[42]

observations suggested that the dual-organelle-targeted AIEgen strategy can effectively improve PDT-chemotherapy, which is reliable for cancer treatment.

Chemotherapeutic drugs could also work as quenchers to silence the PDT effect of AIE PSs. Zhang and Liu *et al.* reported a tetraphenylethylene-thiophene (TPETH) based theranostic probe consisting of two mitochondria-targeted arms decorated with artemisinin (ART).[47] The ART groups showed high selectivity toward tumor cells, two mitochondria-targeted arms could navigate the probe towards mitochondria inside tumor cells, and the TPETH core showed fluorescence once the probe was accumulated in mitochondria. When the probe entered the mitochondria of a tumor cell, heme was generated which activated ART and triggered the generation of ROS. The half
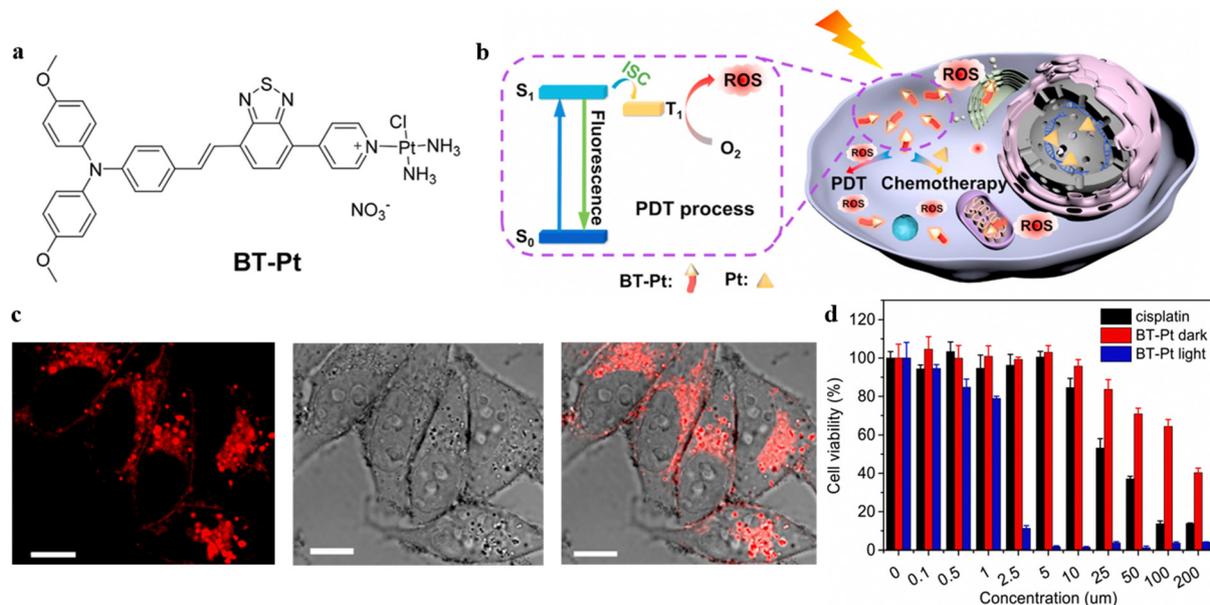
This journal is © The Royal Society of Chemistry 2023

J. Mater. Chem. B, 2023, **11**, 5953–5975 | **5959**

Fig. 5 (a) Molecular structure of BT–Pt. (b) Proposed mechanism of synergistic PDT–chemo theranostics of BT–Pt. (c) CLSM images of HeLa cells after 6 h incubation with BT–Pt (10 μM). Scale bar: 10 μm. (d) The cell viability of HeLa cells pretreated with rising doses of cisplatin and BT–Pt in the presence and absence of white light radiation. Schematic illustration of the proposed mechanism of DOX/ZIF-8 nanoparticles. (D) Reproduced with permission from Elsevier, copyright 2021.[45]

maximal inhibitory concentration (IC_{50}) values toward cancer cells and normal cells indicated the significant tumor killing ability of directing ART to mitochondria. In addition, the mitochondrial membrane was depolarized under the attack of ROS and reduced the migration activity of tumor cells.

Liu *et al.* developed a monitorable therapeutic system TPEPY-S-MMC with a chemo-prodrug mitomycin C (MMC) and PSs TPEPY-SH for traceable combinational PDT-chemotherapy.[48] Only GSH could activate the photosensitizing and chemotherapy, constructing an activatable nanotheranostic with reduced side effects promising for use in personalized medicine. Xia and Yi *et al.* designed a light-trigger decomposable nanoplatform TB/PTX@RTK that was loaded with AIE-PSs (TB) and chemotherapeutic drug PTX, aiming at regulatable drug releases.[49] The TB/PTX@RTK nanoparticle mediated synergistic chemo-PDT effects were assessed both *in vitro* and *in vivo* and demonstrated superior targeting selectivity, chemo-photodynamic "1 + 1 > 2" ablation efficiency, and surprising promotion of antitumor immune responses.

3. Photo-immunotherapy

Traditional cancer immunotherapy utilizes chemical therapy treatments to trigger the immune system to recognize and kill tumors. Cancer immunotherapy advances our understanding on interactions between the immune system and tumors, but it is challenged by a low immune response rate, immunosuppressive mechanisms, and insufficient immunogenicity.[50] Phototherapy can induce the death of cancer cells and express specific antigens to trigger the immune system. Concomitantly,

the target approach combined with immunotherapy can facilitate antigen uptake and presentation, thus stimulating specific antitumor immunity.

3.1. PTT-immunotherapy

Upon light irradiation, PTT can not only ablate cancer cells but also affect the tumor microenvironment (TME): hyperthermia could cause cancer cell death and activate the immune system to inhibit tumor growth.[51] Therefore, the synergy of PTT and immunotherapy has been introduced as an attractive method to enhance cancer therapeutic efficacy with precise imaging, enhanced immunogenicity, and efficient thermal eradication of tumors.

Zhao, Shi, and Tang *et al.* developed a high-performance phototherapeutic nanoconjugate (TPA-NDTA) as displayed in Fig. 7a, which was based on a ferroptosis pathway and could avoid the tumor resistance to apoptosis/necroptosis, generating adequate immunogenicity to induce cancer cell death.[52] The photothermal nanocomposite TPA-NDTA was designed by introducing a molecular rotor with substantial electron donor properties to attain a high photothermal conversion efficiency and broad NIR absorption (from 700 to 1100 nm). TPA-NDTA, aided by photo-hyperthermia (PHT), could perform high efficacy ras-selective lethal small molecule 3 (RSL3)-triggered ferroptosis and advances the effect of immunogenicity in tumors (Fig. 7b). In addition, the mouse model with bilateral tumors showed that locally triggering ferroptosis of the tumor in one side initiated a systemic CD8+ T cell-mediated antitumor immunity and inhibited the tumor growth of distant tumors. The exciting results performed in methyltransferase (MTT) assays and measurements of tumor volume provided a
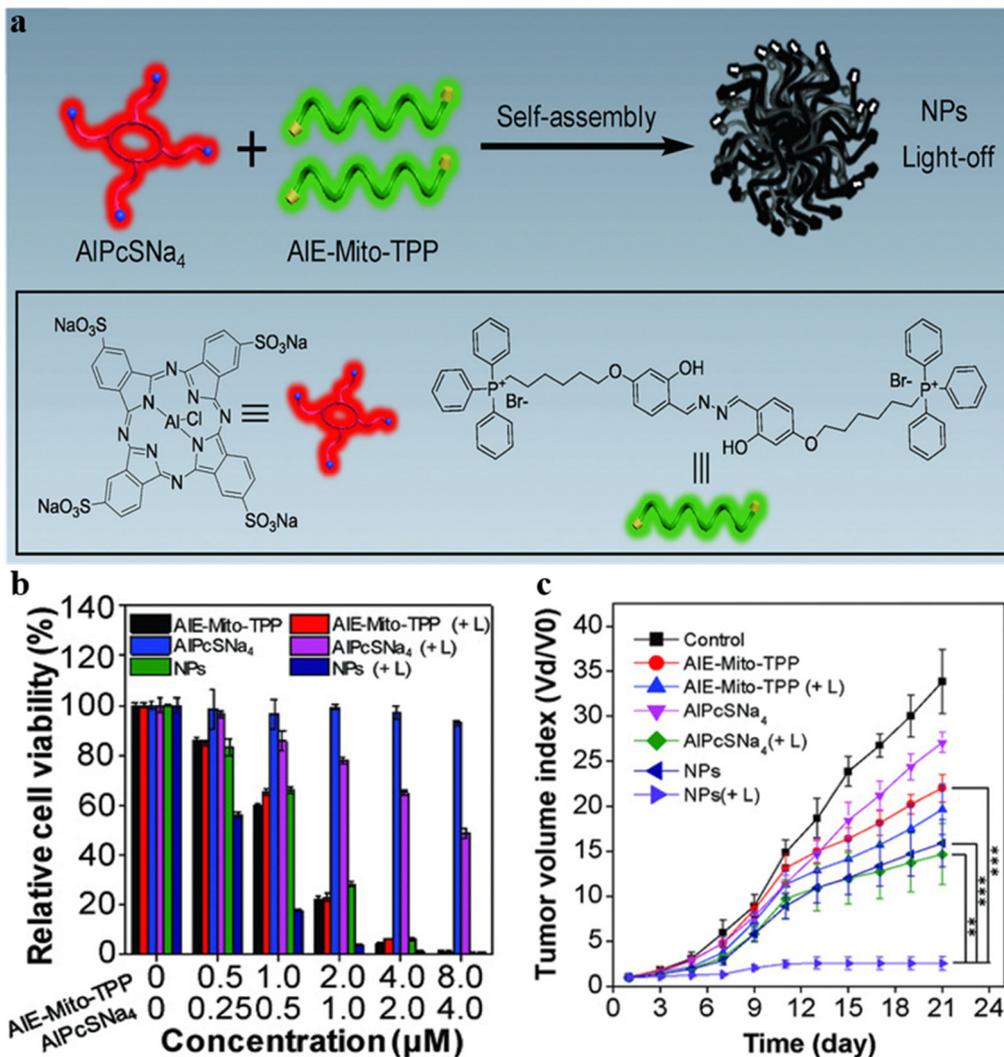
5960 | *J. Mater. Chem. B*, 2023, **11**, 5953–5975

This journal is © The Royal Society of Chemistry 2023

Fig. 6 (a) Designed theranostic AIE-Mito-TPP/AlPcSNa$_4$ nanoparticles. (b) *In vitro* cytotoxicity of AIE-Mito-TPP, AlPcSNa$_4$ and AIE-Mito-TPP/AlPcSNa$_4$ NPs with or without laser irradiation (+L) in A375 cells. (c) The tumor growth curve of tumor-bearing mice under various treatments. Reproduced with permission from Wiley-VCH, copyright 2018.[46]

promising mode for durable antitumor therapy (Fig. 7c and d). This work introduced a strategy of augmenting the immunogenicity of ferroptosis-driven cancer cell death assisted by PHT to improve therapeutic effectiveness.

Peptides are promising for immunotherapy as they can enhance receptor binding affinity and have lower immunogenicity as targeted and therapeutic agents.[53] Wang, Hu, and Wang *et al.* reported the novel peptide-based nanofibers (TAP) containing hydrophobic AIE molecule TPE, which were self-assembled into the nanoparticles with a targeted affinity to programmed death 1 (PD-1) and its ligand PD-L1.[54] The self-assembled peptide-based nanomaterials TAP@TTP could have much better targeting capability for tumor and photothermal conversion efficiency *in vivo* as the TAP@TTP group could afford a higher temperature than the other two comparison groups. Therefore, the self-assembled peptide-based nanomaterials were expected to provide more options for complementary PTT-immunotherapy.

Wang, Yao, and Yu *et al.* synthesized a near-infrared II (NIR-II) emissive molecule TST with AIE property and photothermal effect, which could be used for *in vivo* imaging with deeper tissue penetration depth and higher imaging resolution.[55] TST was further assembled with camptothecin prodrug (CPT-S-PEG) and a new immune checkpoint inhibitor AZD4635, affording the CAT nanoparticles for drug delivery (Fig. 8a). The non-radiation attenuation is inhibited by the strong interaction between CPT and TST, promoting NIR-II fluorescence generation. After entering cancer cells, the CAT nanoparticles disintegrated, and TST were released to exhibit a photothermal effect and enhance non-radiation attenuation (Fig. 8b). The heat generated by TST could induce immunogenic cell death (ICD) of tumor cells and release ATP to recruit immune cells in the TME. To avoid superfluous ATP converting and restricting the immunosuppressive adenosine pathway, the AZD4635 was released by photothermal disintegration, enhancing the immunotherapy effect on tumors. Since ATP can be converted to
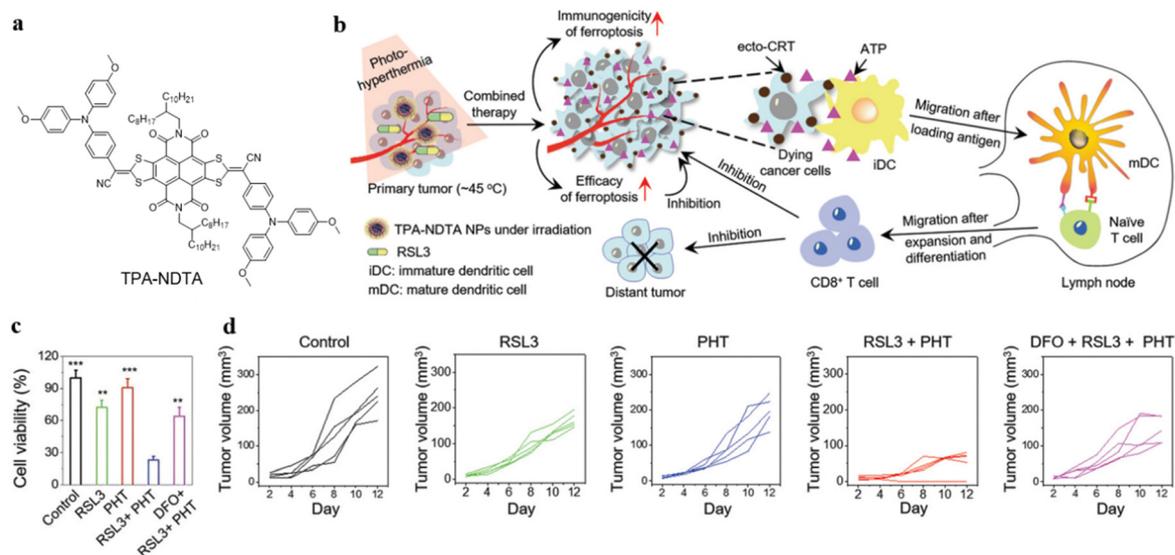
This journal is © The Royal Society of Chemistry 2023

J. Mater. Chem. B, 2023, **11**, 5953–5975 | **5961**

Fig. 7 (a) Molecular structure of TPA–NDTA. (b) Illustration of the mechanism of immunogenic ferroptosis assisted by TPA–NDTA NP-based PHT in a bilateral tumor mouse model. (c) Cell viability of 4T1 cancer cells after various treatments, detected using MTT assay after 24 h. (d) Graphic illustration of the tumor volume of distant tumors after various treatments. Reproduced with permission from Wiley-VCH, copyright 2022.[52]

adenosine which inhibited immune cell activity, the level of ATP and adenosine in MTE was determined by enzyme linked immunosorbent assay (ELISA). Even though CAT-NP could produce the largest amount of ATP, the level of adenosine did not increase in the CAT-NP group and was the lowest of all groups, which demonstrated AZD4635 inhibited the conversion of ATP to adenosine (Fig. 8c and 8d). Therefore, the integration of photothermal and immunotherapy allows the CAT-NP system to inhibit tumor growth effectively.

Zhou, Wang, and Tang *et al.* designed multifunctional AIEgen-based nanoparticles (TPA-BT-DPTQ) as displayed in Fig. 9.[56] The TPA-BT-DPTQ nanoparticles could achieve trimodal NIR-II fluorescence imaging (FLI)/photoacoustic imaging (PAI)/photothermal imaging (PTI). The photoluminescence (PL) of TPA-BT-DPTQ was located at 900–1400 nm with a maximum NIR-II emission peak around 1100 nm. To investigate the antitumor effects of the nanosystem, the measurements of tumor volume *in vivo* of tumor-bearing mice were conducted: compared with all parallel groups, the tumor volumes of mice treated with TPA-BT-DPTQ nanoparticles and exposed to laser irradiation were much smaller. When the cancer cells were treated with TPA-BT-DPTQ nanoparticles, severe 4T1 cell death was observed in Calcein-AM/PI staining images. Therefore, the TPA-BT-DPTQ system could effectively inhibit tumor growth by synergistic PTT-immunotherapy and achieve trimodal imaging-guided cancer theranostics.

3.2. PDT-immunotherapy

PDT can induce the death of tumor cells and release damage-associated molecular patterns (DAMPs) to trigger an immune response in the process of cell death.[57,58] The synergistic PDT-immunotherapy could not only use ROS to kill tumor cells but also activate immune responses by inducing immunogenic cell death to enhance the treatment effect.

Xia, Wang, and Hong *et al.* designed red blood cell (RBC) membrane-packed nanoparticles M@AP.[59] The nanoparticles were constructed by self-assembly of positively charged AIEgen P2-PPh3 and negatively charged Poly(I:C) in a PLGA matrix (Fig. 10a). The nanoparticles accumulated in tumor tissue and were enriched in the spleen due to the homing effect of the RBC membrane, stimulating the immune cells and strengthening the antitumor immune response. Under white light irradiation, the AIE PSs generated ROS to penetrate tumor cells, further promoting tumor antigen (TA) release, and combined with Poly(I:C) to enhance immunity with a synergistic effect (Fig. 10b). In addition, red fluorescence was observed from propidium iodide (PI) staining images, which indicated the antitumor effect of M@AP under light exposure (Fig. 10c). This strategy provides potential treatment for preventing tumor recurrence and metastasis.

Tumor-associated macrophages (TAMs) are joint components of the TME, which could assist tumor progression, invasion, and metastases.[60] TAMs acted as an immunosuppressor to protect the tumor from the immune response. The selective penetration of TAMs could significantly disrupt the TME and improve immunotherapy efficiency. Liu and Tang *et al.* developed a PS, TPE-Man, by decorating TPE with mannose moieties.[61] Since mannose receptors are overexpressed on TAMs, TPE-Man could specifically target TAMs *via* sugar–receptor interaction, allowing fluorescent visualization of TAMs in high contrast and selective eradication of TAMs. Upon exposure to white light irradiation, ROS was generated by the TPE core, and the photodynamic ablation of TAMs was enabled, consequently improving immunotherapy efficiency by modulating the immune microenvironment.
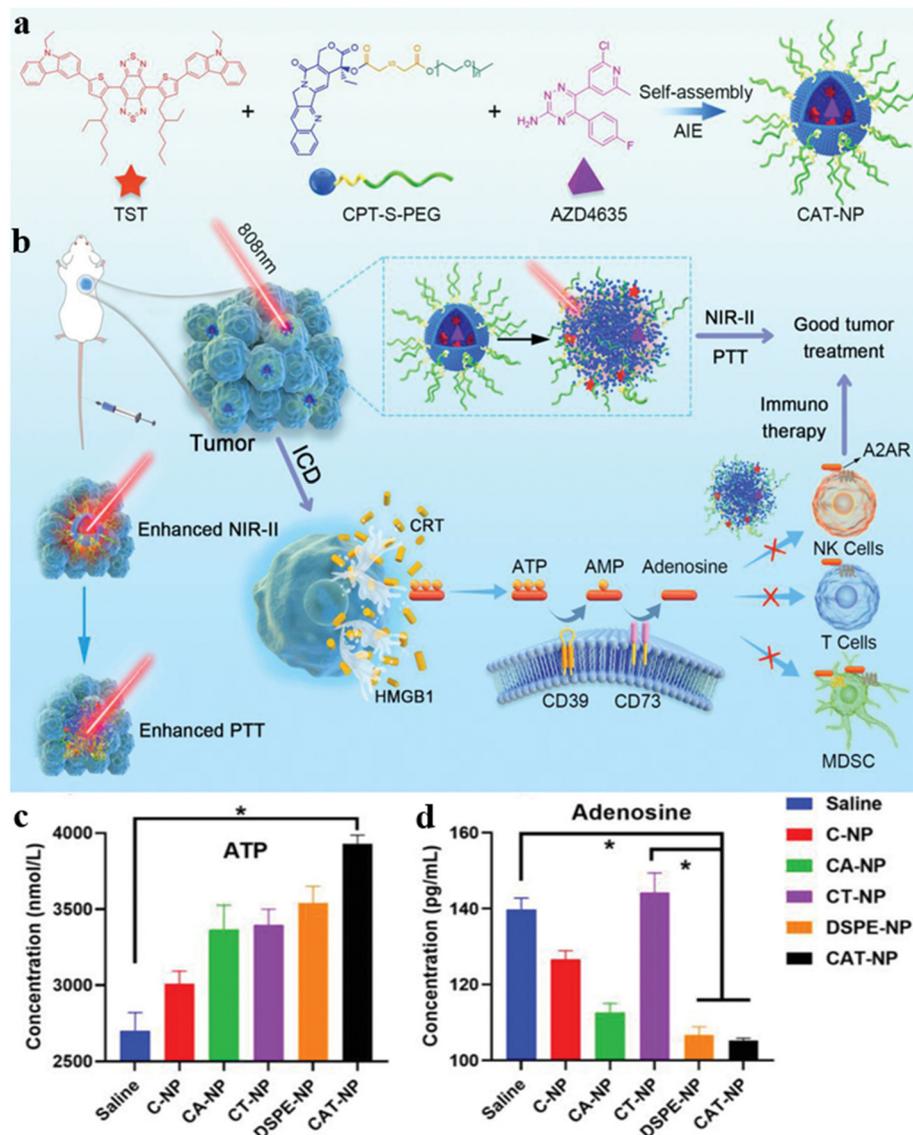
Fig. 8 (a) The assembly of CAT-NP. (b) The schematic illustration of CAT-NP for synergistic PTT-immunotherapy. The determination of content (c) ATP and (d) adenosine in TME. Reproduced with permission from Wiley-VCH, copyright 2022.[55]

Dendritic cell (DC)-derived small extracellular vesicles (DEVs) are an effective alternative to DC vaccines.[62] However, the therapeutic efficacy of DEV-based immunotherapy still needs to be improved. Zhang, Cai, and Tang et al. reported a biomimetic DC@AIEdots system with characteristics of antigen-presenting and hitchhiking.[63] The DC@AIEdots were coated by DC membranes on the AIEgens, and the internal AIE molecules were able to accumulate in the lipid droplets of tumors selectively (Fig. 11a). The tumor delivery efficiency of the photosensitizers was enhanced about 1.6 times because the outer cell membrane facilitated the hitchhiking of DC@AIEdots onto T cells (Fig. 11b and c). The PDT events could kill primary tumors and delay the distant tumors, indicating that tumor proliferation could be effectively inhibited by a strong immune response induced by photo-irradiated DC@AIE dots

(Fig. 11d and 11e). Thus, the DC@AIEdots system demonstrated potential in PDT-immunotherapy.

Wang et al. developed a nanosystem, DEV-AIE nanoparticles, which employed DCs as a cell reactor for exocytosis, achieving synergistic effects of PDT-immunotherapy.[64] The DEV-AIE nanoparticles were exocytosed by the biosynthesis of MBPN-TCyP with DCs. The DEV-AIE nanoparticles could trigger T cell activation due to the immune-modulation proteins from parental DCs. Moreover, the AIE PSs of MBPN-TCyP were loaded onto the nanoparticles to accumulate in mitochondria of tumor cells selectively and induce ICD. Moreover, the DEV-AIE nanoparticles could trigger significant immune responses, eradicate primary tumors effectively, inhibit distant tumors, and suppress tumor metastases. The proposed DEV-AIE nanosystem provided a favorable strategy to prepare clinical anticancer nanovaccines.
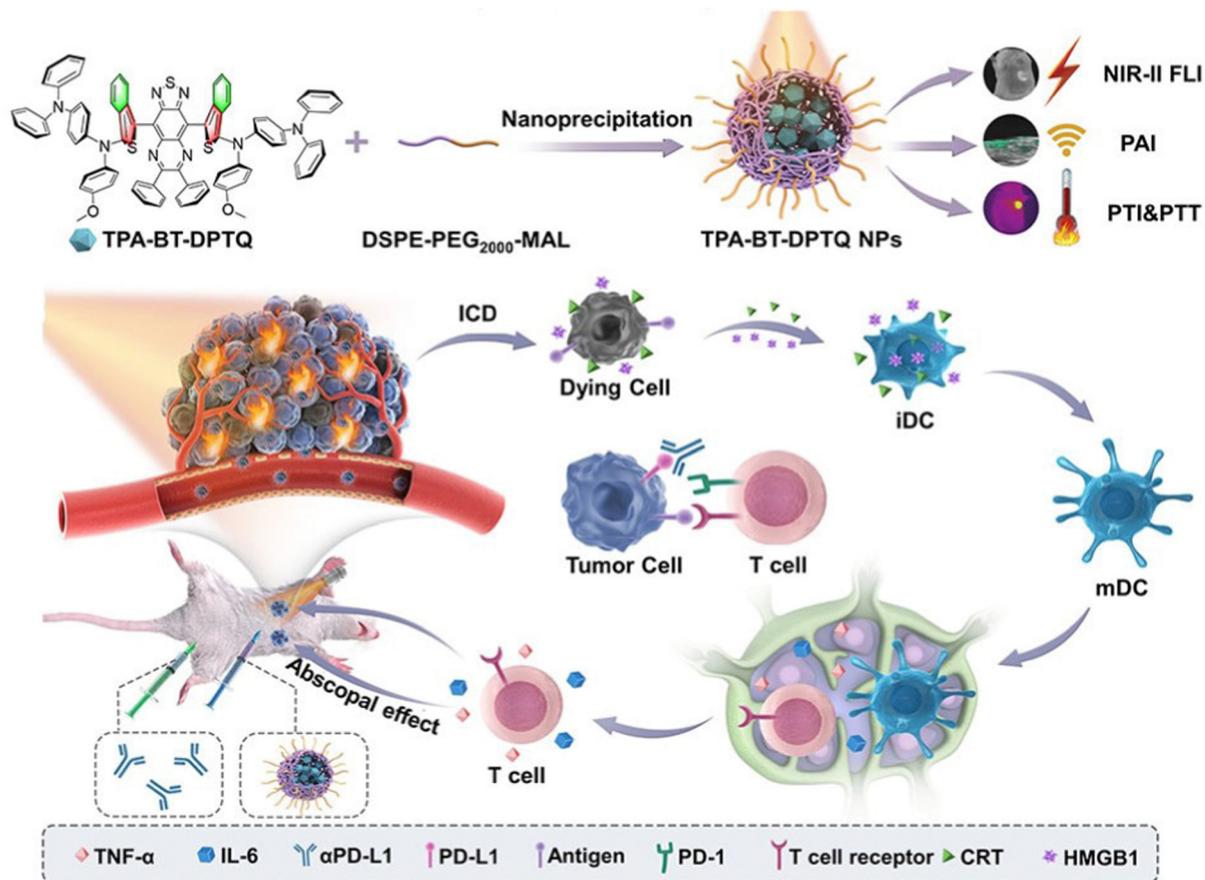
This journal is © The Royal Society of Chemistry 2023

J. Mater. Chem. B, 2023, 11, 5953–5975 | 5963

Fig. 9 Illustration of TPA-BT-DPTQ NPs in synergistic immunotherapy NP-mediated PTT tumor treatment. Reproduced with permission from Wiley-VCH, copyright 2022.[56]
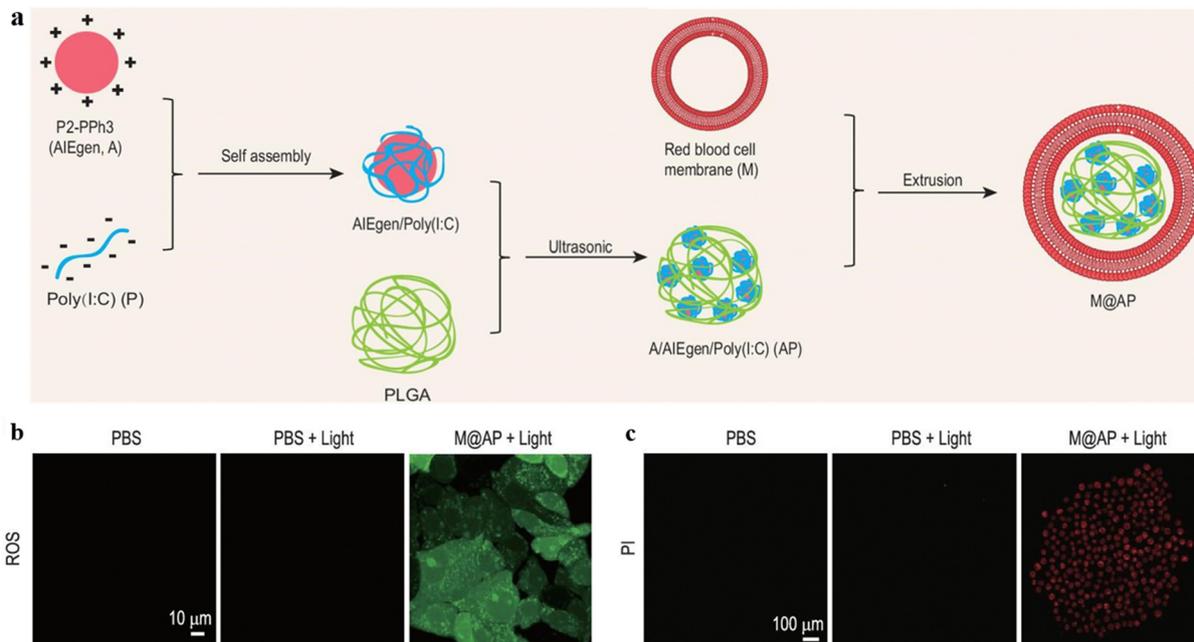

Fig. 10 (a) The preparation of M@AP nanoparticles. (b) The ROS level in B16-F10 cells detected by DCFH-DA (light: 520–540 nm, 100 mW cm^{-2} for 5 min). (c) The cell viability of B16-F10 cells after PDT treatment detected by PI staining (light: 640–680 nm). Reproduced from Oxford University Press, copyright 2021.[59]
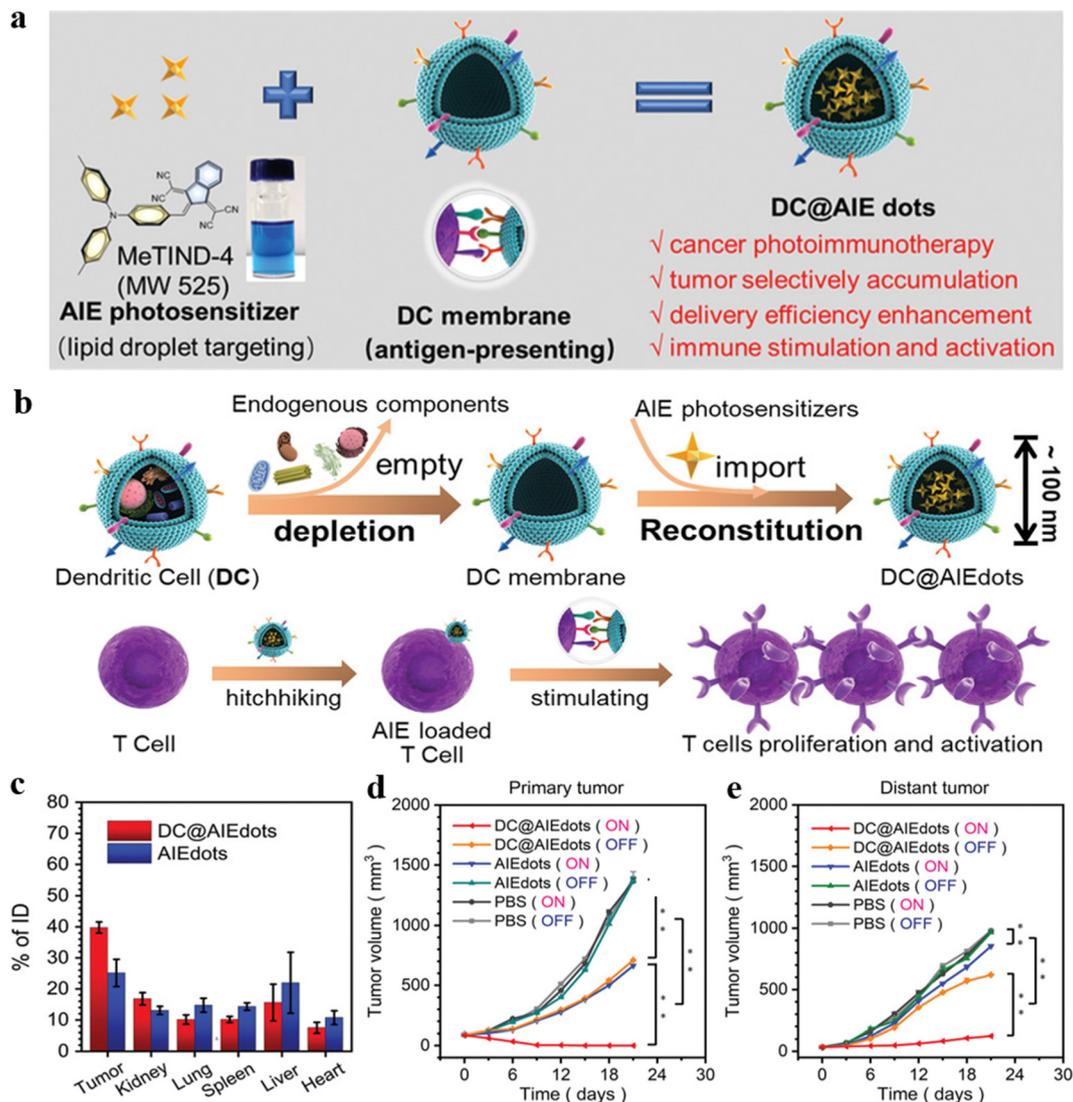
Fig. 11 (a) The assembly of AIE PSs MeTIND-4 coating by DC membrane to form DC@AIE dots. (b) The preparation of DC@AIE dots and the interaction between DC@AIE dots and T cells. (c) Biodistribution measurements of DC@AIE dots or AIE dots after 48 h iv injection in 4T1 tumor-bearing mice. (d) The primary tumor volume and (e) distant tumor volume in different groups after various treatments. Reproduced with permission from Wiley-VCH, copyright 2021.[63]

4. Photo-radiation therapy

Traditional radiation therapy (RT) introduces ionizing radiation to kill cancer cells and inhibit the growth and recurrence of tumors.[65] However, severe damage to normal tissues during RT is usually experienced due to low radiation absorption of tumors and high doses of ionizing radiation. Since phototherapy can effectively intensify the radiation sensitivity of tumor cells,[66] the synergy of RT and phototherapy could enhance the cancer theragnostic effect.

4.1. PTT-radiation therapy

Since radiation therapeutic effectiveness is often limited by severe side effects of excessive radiation doses, a combination of PTT and radiation therapy allows radiation therapy to kill tumor cells under a lower radiation dose.[67,68] In addition,

hyperthermia caused by PTT could directly enhance antitumor effects and intensify hypoxic sensitivity of tumor cells.

Tang *et al.* presented a novel strategy for multimodal imaging and PTT-radiation synergistic therapeutics with silver core/AIE shell nanoparticles.[69] The nanoparticles were prepared *via* redox reaction between TPE-M2OH and Ag^+, and the nanoparticles are further coated by TPE-M2OH through donor–acceptor interactions (Fig. 12). The nanoparticles not only demonstrated inherent AIE FLI, metal-based computed tomography (CT), and RT properties, but also exhibited functionality of good photothermal (PT) and PAI performance at the core/shell interface. Consequently, the three imaging modalities (FLI, CT and PAI) and synergistic PTT-radiation treatment were combined within a single structural unit for accurate tumor imaging and therapy. The cell viability *in vitro* decreased to 19% at an AACSN concentration of 1.0 mg mL^{-1}. The tumor
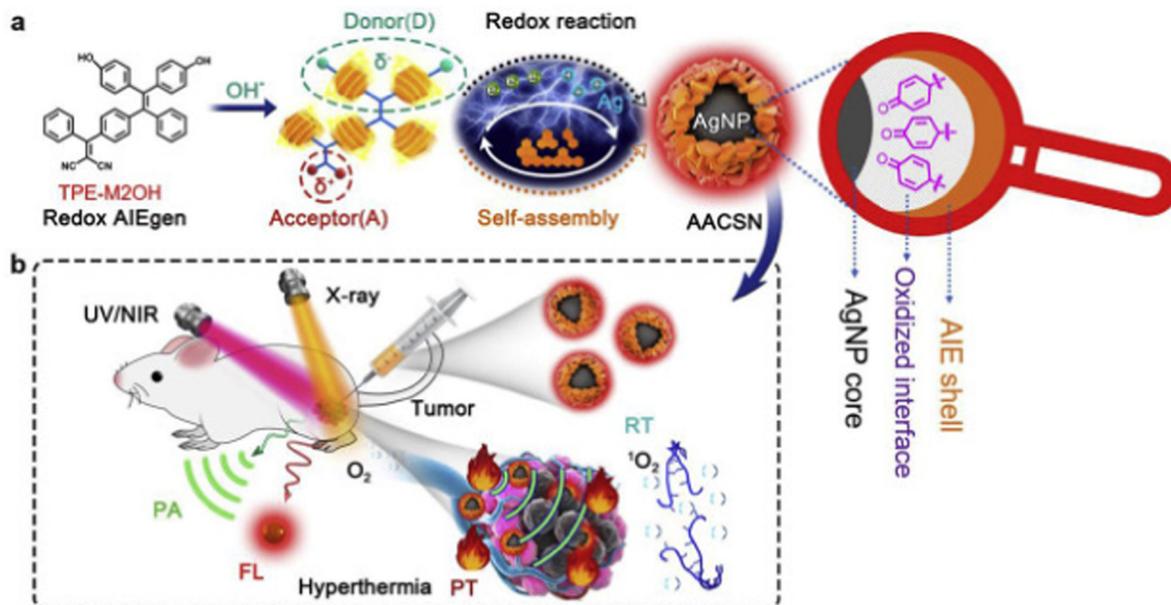
Fig. 12 (a) AACSN synthesis *via* the redox reaction between Ag+ and TPE-M2OH and the self-assembly of AIEgens with a D−A structure. Oxidized interface layer with quinone structures between the AgNP core and AIE shell was *in situ* generated through the redox reaction. This new functionality is assigned to the origin of PT and PA properties. (b) AACSNs were applied for five-modality tumor imaging (FL, PT, PA) and synergistic PTT and RT therapy. Reproduced with permission from Elsevier, copyright 2020.[69]

growth *in vivo* was significantly inhibited, and the 30 day survival rate of mice increased to 100% under "AACSN + PTT + RT" treatment. The proposed nanosystem based on a "less is more" strategy constructed a simple core@shell nanoparticle and achieved multi-modal imaging synergistic PTT-radiation cancer therapy. Cai and Han *et al.* also constructed a multifunctional imaging-guided PTT-radiation cancer therapy based on AIEgen (TPA-BT-DPTQ), which could thermally ablate tumors and achieve multimodal imaging.[70] The gold nanorod (GNR)-mediated nanoagents (NPAPF-GNRs@PEG) were engineered with AIEgen TPA-BT-DPTQ to achieve PTT-radiation synergistic therapy, and the nanoplatform demonstrated photothermal-enhanced radiation effects and an efficient capacity for killing primary and distant tumors, effectively preventing recurrence of cancers. The NPAPF-GNRs@PEG nanosystem achieved multi-modal (CTI/PAI/FLI/PTI) imaging-guided and photothermal-enhanced radiation therapy *in vivo*.

4.2. PDT-radiation therapy

Radiation therapy directly kills tumor cells by exposing the tumor issue to high-energy radiation. Theoretically, the tumor can be destroyed under a significant radiation dose. However, the radiation has a strong penetrability and might cause severe lesions to the surrounding healthy tissue.[71] Specific PDT agents can enhance the radiation sensitivity of tumor cells, consequently reducing the required dose of radiation treatment. Combining PDT and radiation therapy could reduce radiation side effects and improve the therapeutic efficacy.

Li, Ding, and Tang *et al.* reported an AIE-based method to promote the radiosensitivity of tumor cells.[72] A mitochondria-targeted PS DPA-SCP was constructed by connecting an AIE core with pyridinium salt (Fig. 13a). DPA-SCP could selectively accumulate in mitochondria, generate fluorescence, and generate $^1O_2$ under white light irradiation. The $^1O_2$ generation in tumor cells could significantly promote radiosensitivity of cancer cells and inhibit the phosphorylation of Akt and ERK in tumor cells to induce apoptosis. Consequently, the sensitizer enhancement ratio at 10% cell survival rate (SER10) value was 1.62, which was higher than those of the popular radiosensitizers of Au nanoparticles and paclitaxel (Fig. 13b).

Zheng and Tang *et al.* reported an AIE PS based on triphenylamine and azafluorenone, TPANPF$_6$ (Fig. 14a), with outstanding photodynamic properties compared with the other three derivatives.[73] The cationization of the core enhanced the
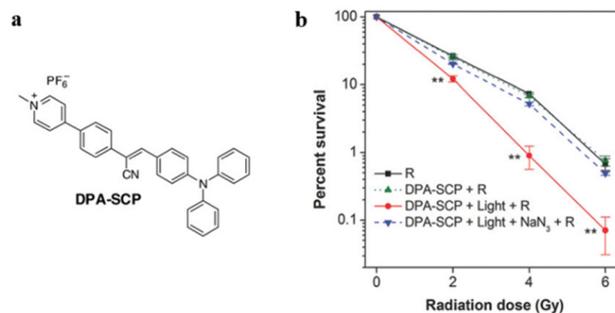

Fig. 13 (a) The chemical structure of DPA-SCP. (b) Survival rate of A549 cancer cells after various treatments. Reproduced with permission from Wiley-VCH, copyright 2017.[72]
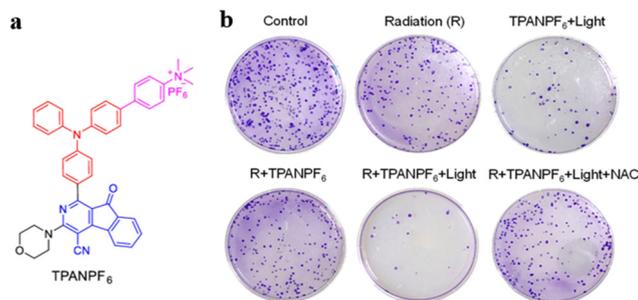
5966 | *J. Mater. Chem. B*, 2023, **11**, 5953–5975

This journal is © The Royal Society of Chemistry 2023

Fig. 14 (a) The chemical structure of TPANPF$_6$. (b) Photographs of colony formation under various treatments. Reproduced with permission from American Chemical Society, copyright 2019.[73]

ROS generation efficiency and the mitochondria-targeting ability of the PSs. The PSs showed poor solubility and high aggregation degree in aqueous solutions and achieved good ROS generation and fluorescence. As a radiosensitizer, TPANPF$_6$ demonstrated excellent enhancement in radiation therapy efficiency. The data of colony development indicated that the "radiation + TPANPF$_6$ + light" exhibited more significant inhibitory effects on the tumor colony formation than radiation and "TPANPF$_6$ + light" alone (Fig. 14b). The cationized mitochondria-targeting PSs indicated cationization as a potential strategy to improve ROS generation efficiency, and the synergy of PDT and radiotherapy improves cancer therapeutic efficiency.

Chen *et al.* designed AIE-based clustoluminogens (AIE-Au) for low-dose X-ray-induced PDT (X-PDT) to achieve synergistic PTT-radiation therapy with reduced side effects.[74] The consequent aggregation of AIE-Au enhanced the X-ray luminescent emission by 5.2-fold. Under low-dose X-ray irradiation, the AIE-Au significantly absorbed X-ray and generated abundant OH$^\bullet$ radicals, which enhanced the radiosensitivity of targeted cells and promoted the radiotherapy effect. Meanwhile, the X-ray luminescence further excited the conjugated PSs, resulting in a photodynamic effect. The *in vitro* and *in vivo* experiments implied that AIE-Au efficiently triggered ROS generation with
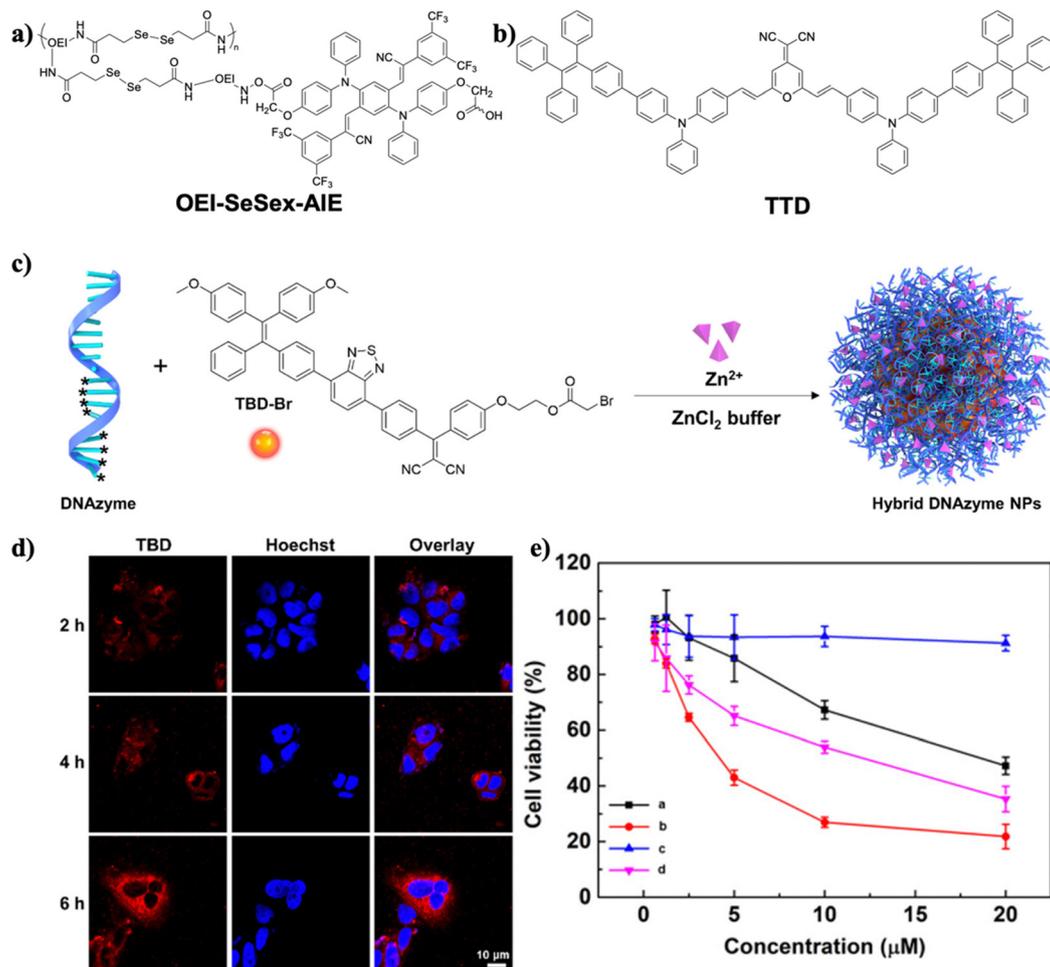

Fig. 15 (a) The chemical structure of OEI-SeSex–AIE. (b) The chemical structure of TTD. (c) Illustration of preparing hybrid DNAzyme nanoparticles. (d) Confocal fluorescence images of MCG-7 cells after incubating with DNAzyme-mediated nanoparticles. (e) Cytotoxicity tests of MCF-7 cancer cells *in vitro* after various treatments ((a): hybrid DNAzyme nanoparticles; (b): hybrid DNAzyme nanoparticles under light irradiation; (c): TBD nanoparticles under dark conditions; (d): TBD nanoparticles under light irradiation). Reproduced with permission from American Chemical Society, copyright 2021.[79]

This journal is © The Royal Society of Chemistry 2023

J. Mater. Chem. B, 2023, **11**, 5953–5975 | **5967**

a considerable proportional reduction in X-ray dose, which reduced side effects and promoted treatment efficiency.

5. PDT–gene therapy

Gene therapy traditionally uses small interfering RNA (siRNA) to knockdown the target gene's expression for gene silencing. Nevertheless, it is limited by low gene transfer efficiency and the selection of gene delivery vectors.[75] Some cases of combining PDT and gene therapy have been introduced as an effective strategy to improve anticancer therapeutic effectiveness.

Gao *et al.* developed a gene delivery system consisting of a ROS-labile diselenide linkage and an AIEgen.[76] The proposed system could achieve unprecedented $^1O_2$ production efficiency (80.14%). Under daylight irradiation, the internalized plasmid DNA (pDNA) self-assembled into AIE nanoparticles, forming OEI-SeSex-AIE (Fig. 15a). Meanwhile, daylight irradiation could elicit ROS-labile diselenide bond cleavage and destabilize the structure of AIE nanoparticles to release pDNA. As a result, the proposed delivery system exerted self-sufficient ROS production to facilitate endosomal escape, thus greatly improving gene delivery efficiency.

Cancer cells can induce angiogenesis to resist ROS generation by upregulating the expression of vascular endothelial growth factor (VEGF), resulting in attenuation of the PDT effect.[77] To address the resistance issue, Liu and Li *et al.* reported a combination of surface siRNA decoration and AIE-gens for PDT and RNA interference therapy synergy.[78] The siRNA played a crucial role in inhibiting VEGF expression. 2-(2,6-bis((E)-4-(phenyl(40-(1,2,2-triphenylvinyl)-[1,10-biphenyl]-4-yl)amino)styryl)-4H-pyran-4-ylidene)malononitrile (TTD), as shown in Fig. 15b, was employed as the AIE PS to generate ROS under light irradiation, yielding bright fluorescence, high phototoxicity, high spatiotemporal accuracy, and precise controllability. The nanoparticles' surface was decorated with small interfering RNA-vascular endothelial growth factor (siVEGF) and cRGD to integrin-overexpressed cells and delivered siRNA. Thus, this anticancer system achieved a synergistic PDT-RNA interfering therapeutic effect.

Gao and Liu *et al.* constructed a light-induced carrier-free DNAzyme delivery system.[79] DNAzymes are more stable in a biological environment without hijacking the endogenous RNA-induced pathway relative to siRNA.[80] TBD-Br was fabricated onto hybrid DNAzyme nanoparticles with the thiophosphate group in order to become amphiphilic and to enhance
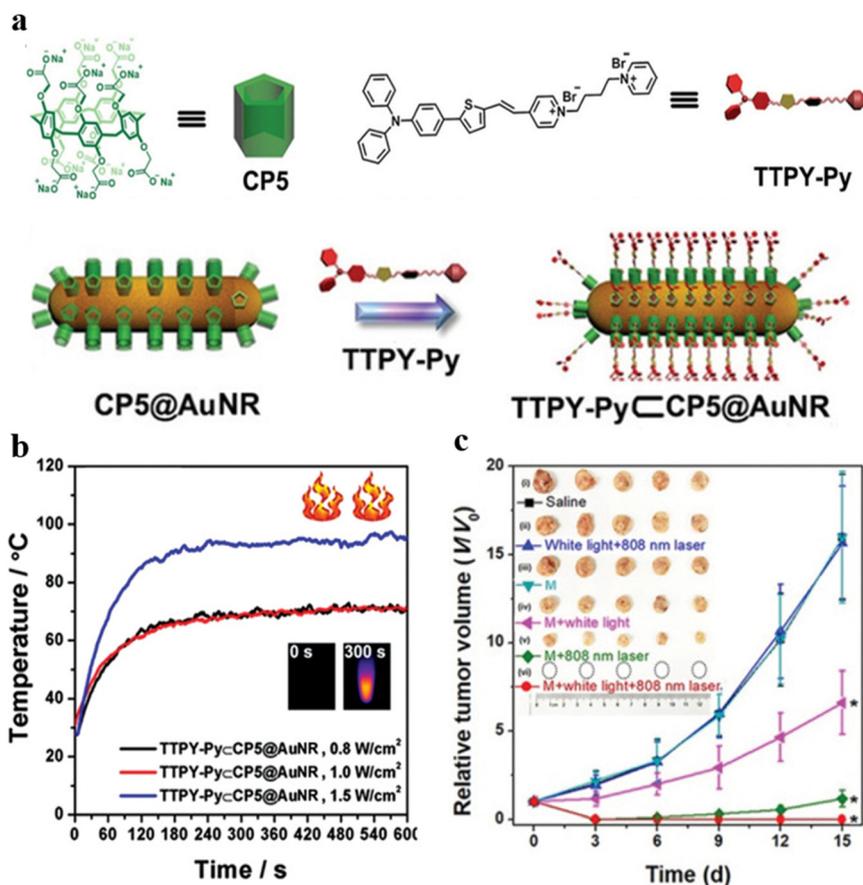

Fig. 16 (a) The chemical structure of CP5 and TTPY-Py and the preparation of TTPY-Py ⊂ CP5@AuNR. (b) Photothermal property of TTPY-Py ⊂ CP5@AuNR under various powers of 808 nm laser. (c) Tumor volumes of 4T1 tumor-bearing mice after various treatments. Reproduced with permission from Wiley-VCH, copyright 2021.[85]

5968 | *J. Mater. Chem. B*, 2023, **11**, 5953–5975

This journal is © The Royal Society of Chemistry 2023

the ROS generation efficiency and fluorescence intensity, forming hybrid DNAzyme nanoparticles (Fig. 15c). DNAzyme-based spherical nucleic acids (SNA) were employed as ligands to obtain a high encapsulation rate of cofactor (Zn^{2+}) and tackle the insufficient metal ion coenzyme supply. When the hybrid DNAzyme nanoparticles entered cancer cells, the AIEgen TBD-Br induced the production of $^1O_2$ under light irradiation to destroy the lysosome structure and help hybrid DNAzyme nanoparticles escape from lysosomes. The red fluorescence emitted from TBD could be observed as shown in Fig. 15d, demonstrating successful cellular uptake of hybrid DNAzyme nanoparticles in MCF-7 cells. The cytotoxicity analysis indicated the antitumor effects of hybrid DNAzyme nanoparticles (Fig. 15e). As a result, the hybrid DNAzyme nanoparticles could generate $^1O_2$ to induce tumor cell apoptosis under light irradiation as well as regulate the expression of the early growth response factor-1 protein (EGR-1) mRNA to inhibit tumor cell growth. Therefore, the DNAzyme-mediated conjugate with TBD-Br achieved the synergistic effect of PDT-gene therapy. Zhao, Lou, and Xia *et al.* developed a GSH-responsive MnO_2-DNAzyme-TB (MDT) nanocomposite for cancer imaging and PDT-gene synergistic therapy.[81] While TB acted as an AIE photosensitizer, DNAzyme was employed to catalyze degradation of EGR-1 mRNA and to silence the gene. When internalized into cancer cells, MDT nanoparticles could downregulate the

expression of EGR-1 to suppress cell growth. Additionally, the aggregated TB can produce $^1O_2$ to destroy cancer cells further. The MDT system thus inhibited cancer cell growth by synergistic gene silencing and PDT.

6. Other synergistic therapy

6.1. PTT–PDT

PTT and PDT have emerged as safe and secure ways to destroy established tumor cells, whereas single PDT or PTT is not enough to realize high treatment efficiency.[82] To achieve the maximized therapeutic effects, synergistic theranostics of PTT and PDT have been developed to compensate for each method's defects.

Integrating host–guest interactions with AIEgens can facilitate the modulation of photo-related properties.[83,84] Yang, Wang, and Tang *et al.* constructed versatile theranostic nanocomposites TTPY-Py ⊂ CP5@AuNR based on host–guest interactions for synergistic PTT–PDT.[85] Au nanorods (AuNRs) possessed an photoacoustic feature, and the surfaces of AuNRs were further modified by supramolecular building blocks to decrease cytotoxicity and increase the dispersibility of AuNRs (Fig. 16a). TTPY-Py ⊂ CP5@AuNR exhibited high photothermal conversion efficiency due to rod-like shape and surface electron
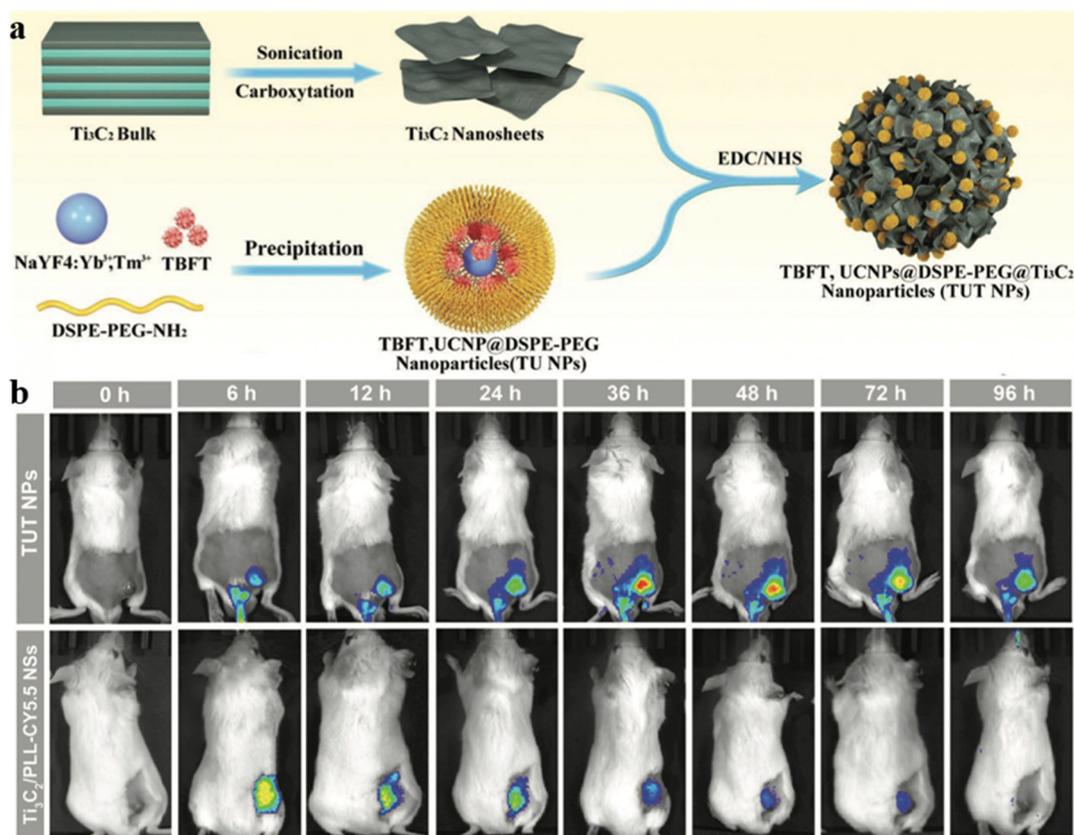

Fig. 17   (a) The preparation of TUT nanoparticles. (b) NIR FLI of tumor-bearing mice taken at different periods after injection of TUT nanoparticles or Ti₃C₂/PLL-CY5.5 nanosheets. Reproduced with permission from Wiley-VCH, copyright 2022.[87]

This journal is © The Royal Society of Chemistry 2023

J. Mater. Chem. B, 2023, **11**, 5953–5975 | **5969**

resonance of AuNRs (Fig. 16b). TTPY-Py serves as PS with AIE characteristics that can target mitochondria and generate ROS for PDT. TTPY-Py $\subset$ CP5@AuNR can achieve synergistic PTT–PDT antitumor effects upon the irradiation of both white light and NIR laser (Fig. 16c). The TTPY-Py $\subset$ CP5@AuNR phototheranostics can thus achieve therapeutic goals with precise dual-modal-imaging-guided (FLI-PAI) synergistic PTT–PDT treatment. Wang et al. constructed the supramolecular complex with a similar strategy to achieve synergistic PDT-chemo therapy.[86]

Wang and Tang et al. reported a multifunctional nanosystem (TUT nanoparticles), as shown in Fig. 17a, comprised of early-transition-metal carbides (MXenes), AIE-active PSs, and upconversion nanoparticles (UCNPs) for cancer phototheranostics.[87] Typical MXenes, Ti_3C_2 nanosheets were employed due to their outstanding photothermal conversion efficiency and high absorption ability in the long-wavelength region, while UCNPs were used to extend the excitation wavelength of the AIE-active PSs (TBFT) via a Förster resonance energy transfer (FRET) process.[88–90] The resulting TUT nanoparticles were covalently bonded, giving efficient tumor accumulation with better physiological stability in vivo and in vitro assessment. As shown in Fig. 17b, TUT nanoparticles outperform the Ti_3C_2/PLL-CY5.5 nanosheet group in tumor accumulation, as the covalently bonded surface makes TUT nanoparticles

impregnable in the physiological environment. Based on the aggregation-enhanced FLI/PAI/PTI guided synergistic PTT–PDT, the TUT nanoparticles exhibited high antitumor efficacy and further encouraged the exploration of inorganic–organic nanocomposites for synergistic anticancer therapy.

6.2. Multimodal therapy

Multimodal synergistic therapies have been developed to make up for the defects of individual approaches and integrate their collective advantages to improve treatment efficacy.[91] Wang and Tang et al. reported an acidic TME-activatable nanosystem, AD-Cu-DOX-HA as displayed in Fig. 18.[92] Due to capping of hyaluronic acid (HA), the AIEgen MeOTTVP could be selectively activated, proposing a promising strategy for the formation of intelligent aggregates. The nanosystem could precisely distinguish cancer cells from normal cells; additionally, it possessed multiple functions including high-performance ROS generation, selective accumulation, Cu^{2+} mediated rapid decomposition, and activable fluorescence in tumor tissue simultaneously. Consequently, AD-Cu-DOX-HA demonstrated efficient tumor diagnosis and tumor-growth inhibition through FLI-navigated synergistic therapy of stimuli-responsive chemotherapy, Cu^{2+}-mediated chemodynamic therapy (CDT), and PDT.
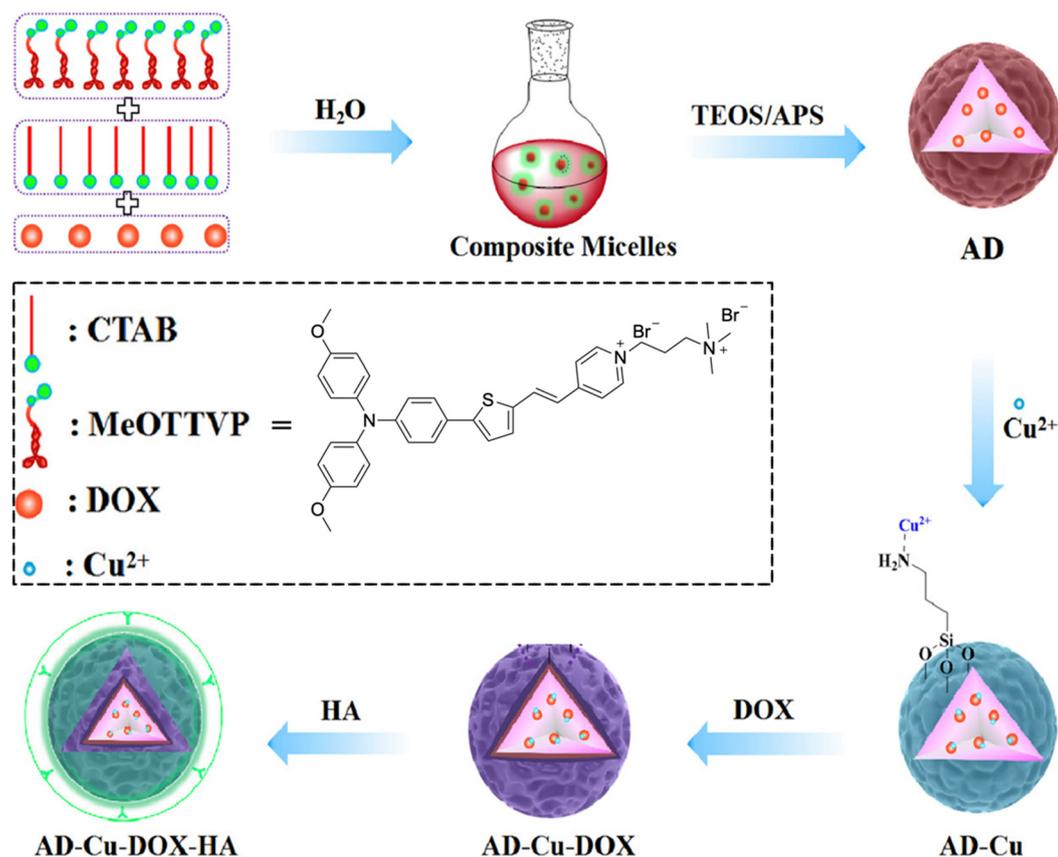

Fig. 18 The chemical structure of MeOTTVP and the preparation process of AD-Cu-DOX-HA nanosystems. Reproduced with permission from American Chemical Society, copyright 2022.[92]

5970 | J. Mater. Chem. B, 2023, 11, 5953–5975

This journal is © The Royal Society of Chemistry 2023

Even though multimodal therapy can enhance cancer therapeutic efficiency, it usually requires complicated parameters to construct the theranostic system. Zhao, Lou, and Tang *et al.* effectively designed a novel versatile nanosystem based on a single AIEgen, DDTB as displayed in Fig. 19a, to integrate NIR fluorescence, immunotherapy, PTT, and PDT.[93] The proposed nanosystem can be used for preoperative diagnosis as the nanoparticles accumulate in tumors with NIR fluorescence. In addition, DDTB-DP nanoparticles held great potential as a NIR-II FLI probe (Fig. 19b). The fluorescence intensity of the nanoparticles at the tumor site increased over time to a maximal level at 24 h post-injection (Fig. 19c). DDTB-DP nanoparticles can effectively inhibit tumor progression when combined with PD-L1 antibody and laser irradiation (Fig. 19d and e). No significant weight loss of tumor-bearing was observed, indicating the low systematic toxicity of the nanoparticles (Fig. 19f). PTT–PDT combined with PD-L1 antibody significantly suppresses tumor growth by heightening the immunotherapy effect.

The design of NIR-II fluorescence imaging is receiving more and more attention due to its higher penetration depth, weaker light damage to normal tissues, and lower autofluorescence.[94–98] Tang and Wang *et al.* constructed an AIE-active supramolecular metallacage with fluorescence imaging at the NIR-II region for the first time.[99] The M_6L_3-type metallacage C-DTTP exhibited AIE properties and photothermal conversion and ROS generation (Fig. 20a). The maximum emission length can reach 1005 nm, which is the longest fluorescence emission compared with previously reported fluorescent supramolecular coordination complexes and allows C-DTTP to achieve NIR-II fluorescence/photothermal dual-imaging-guided synergistic PDT-PTT cancer theranostics. The metallacage and its ligands were encapsulated into mPEG-
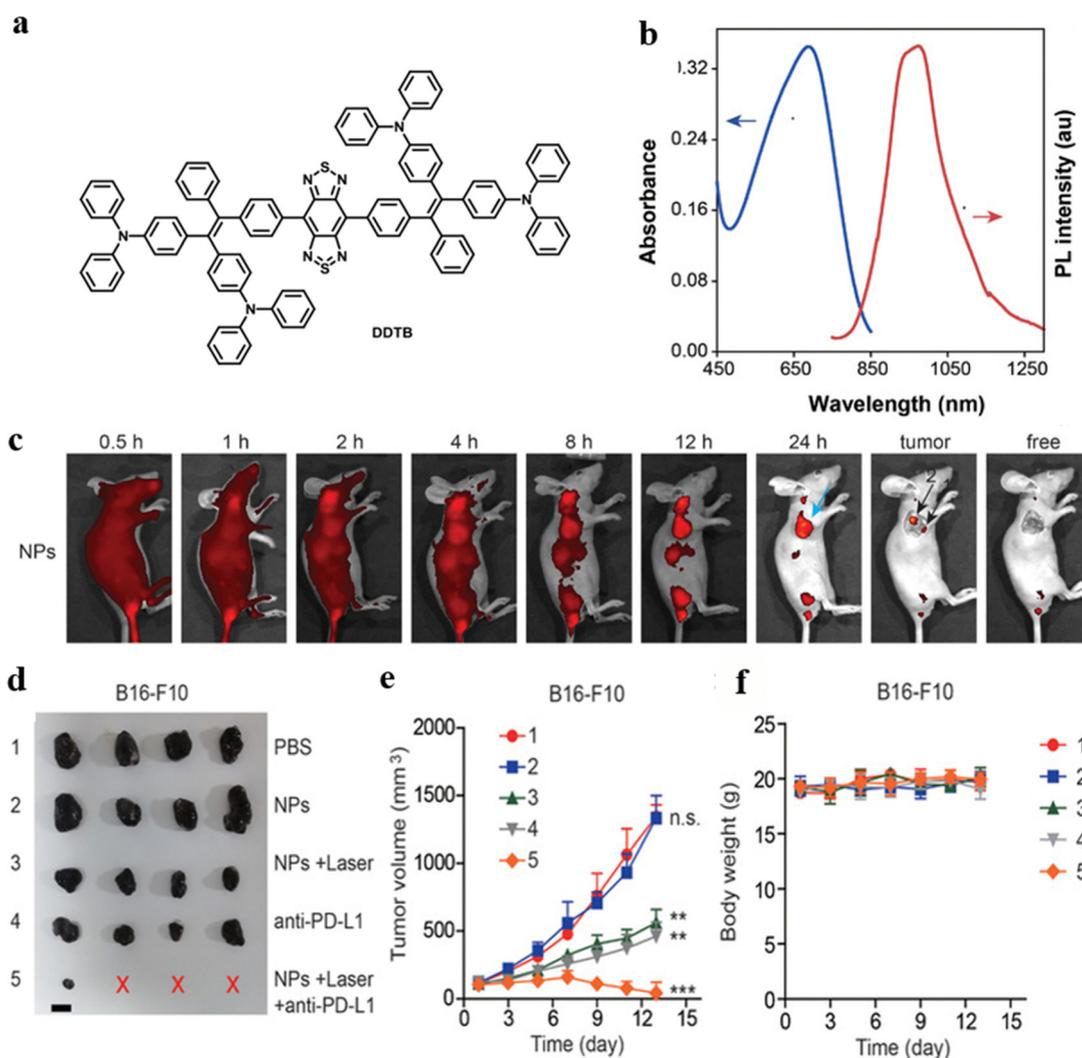

Fig. 19 (a) The chemical structure of DDTB. (b) Absorption and emission spectra of DDTB–DP nanoparticles in aqueous solution. (c) *In vivo* fluorescence images of HeLa tumor-bearing mice after various time periods of intravenous injection of DDTB–DP nanoparticles. (d) Tumor images of B16-F10 tumor bearing mice after various treatments (the red X indicated no tumor was detected). (e) Tumor volume growth curves of B16-F10 tumor bearing mice after various treatments. (f) Measurements of the body weight of B16-F10 tumor bearing mice after various treatments. Reproduced with permission from Wiley-VCH, copyright 2021.[93]
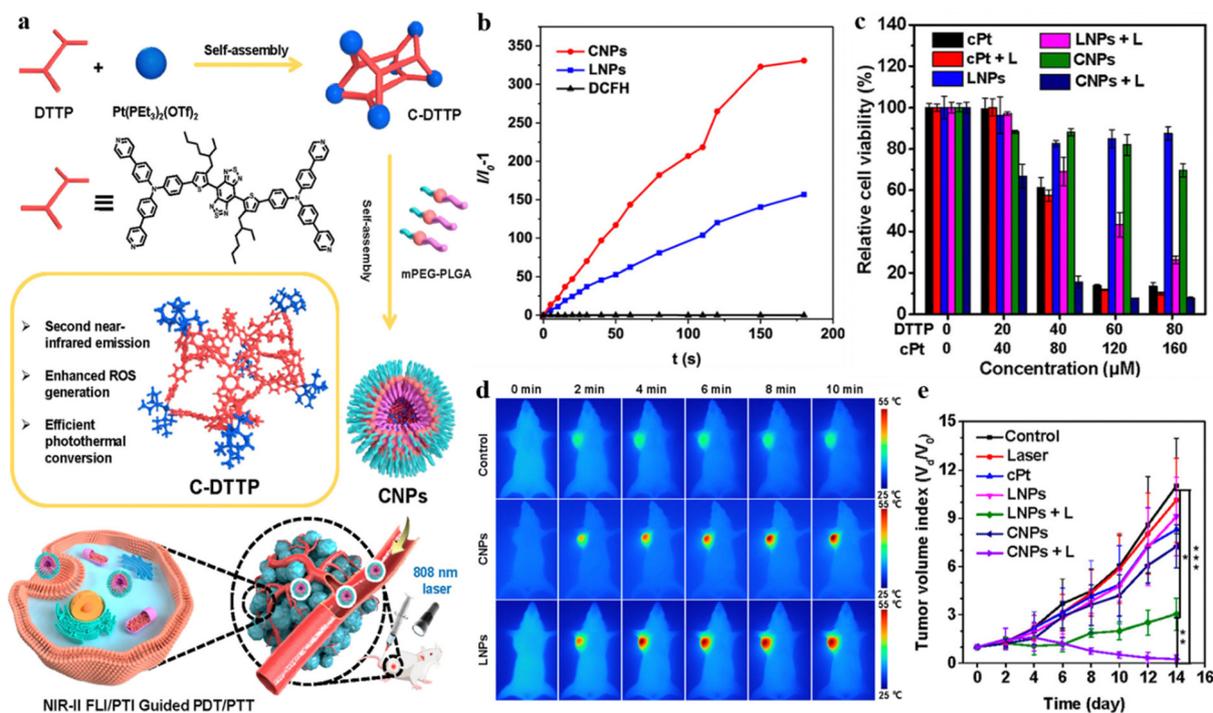
This journal is © The Royal Society of Chemistry 2023

J. Mater. Chem. B, 2023, **11**, 5953–5975 | **5971**

Fig. 20 (a) The designed C-DTTP metallcage. (b) ROS generation of LNPs and CNPs exposed to an 808 nm laser. (c) Cell viability of MDA-MB-231 cells after various treatments (L: 808 nm laser irradiation). (d) Thermal images of MDA-MB-231 tumor-bearing mice with different treatments. (e) Tumor volume growth curves of tumor-bearing mice with different treatments. Reproduced with permission from American Chemical Society, copyright 2022.99

PLGA, respectively, to form CNPs and LNPs to test the applicability of the designed supramolecular system in biological applications. The performance of ROS generation can be better in CNPs than in LNPs under 808 nm laser irradiation (Fig. 20b). CNPs displayed greater temperature evaluation in thermal images, indicating the excellent photothermal conversion efficiency of CNPs *in vivo* (Fig. 20d). The cancer cell viability decreased remarkably when CNPs were exposed to laser irradiation compared to CNPs alone and LNPs under irradiation, and the tumor growth was suppressed when the tumor-bearing mice were treated with CNPs and irradiation, proving the antitumoral capability of the designed PTT–PDT synergistic theranostics (Fig. 20c and e).

Zhao *et al.* synthesized NIR AIEgen-based fluorophore TACQ with mitophagy regulating activity for mitochondria-targeted cancer theranostics.[100] The TACQ AIEgen was based on a donor–acceptor structure and had a longer emission in the NIR-II window due to the strong push–pull effect. Concurrently, the rotor structure and twisted molecular conformation enabled TACQ to balance the nonradiative and radiative energy dissipation, resulting in efficient ROS generation, high photothermal conversion efficiency, and high quantum efficiency, which could be employed in synergistic therapy. The lipocationic property of TACQ allowed the nanothernostics to selectively target the mitochondria of cancer cells, trigger mitophagy, and inhibit mitophagy flux. Both *in vitro* and *in vivo* experiments demonstrated that the theranostic platform based on TACQ was promising for mitochondria-targeting with NIR FLI and

PTI-guided synergistic chemo-PTT–PDT. The satisfying therapeutic efficiency indicated the future trend of combining more than two approaches to improve the therapeutic efficiency.

7. Conclusions and outlook

AIEgen-based synergistic cancer therapy has captured significant attention to maximize therapeutic effectiveness by integrating collective capacities and making up for deficiencies of each approach. This review summarized recent advancement of AIEgen-based synergistic cancer therapy, which is based on the combination of phototherapy with other therapeutic modalities to construct a multifunctional nanoplatform for precise tumor treatments. Although AIEgen-based synergistic anticancer theranostic systems have obtained colossal progress, there are still challenges to be tackled before practical application. First, the absorption and emission range of AIEgens should be further expanded; more AIEgens with NIR-II-range emission need to be developed to cater for *in vivo* imaging with a higher penetration depth and signal-to-noise ratio. Second, further investigation in incorporating various therapeutic modalities into one single nanoplatform can be conducted to improve theranostic efficacy and reduce drug resistance. Third, a reduction in phototoxicity is urgently needed to minimize adverse effects and prevent damage to healthy tissues. Fourth, the design of photosensitizers which can generate ROS in a hypoxic environment holds promising potential in cancer theranostics. Even though there

5972 | *J. Mater. Chem. B*, 2023, **11**, 5953–5975

This journal is © The Royal Society of Chemistry 2023

are some challenges, the AIEgen-based synergistic anticancer therapy is promising for the future development of cancer treatment in preoperative diagnosis and optical theranostics. We hope more innovative ideas and breakthroughs in this emerging field can be inspired by this review.

Conflicts of interest

There are no conflicts to declare.

Acknowledgements

References

1 W. G. Jiang, A. J. Sanders, M. Katoh, H. Ungefroren, F. Gieseler, M. Prince, S. K. Thompson, M. Zollo, D. Spano, P. Dhawan, D. Sliva, P. R. Subbarayan, M. Sarkar, K. Honoki, H. Fujii, A. G. Georgakilas, A. Amedei, E. Niccolai, A. Amin, S. S. Ashraf, L. Ye, W. G. Helferich, X. Yang, C. S. Boosani, G. Guha, M. R. Ciriolo, K. Aquilano, S. Chen, A. S. Azmi, W. N. Keith, A. Bilsland, D. Bhakta, D. Halicka, S. Nowsheen, F. Pantano and D. Santini, *Semin. Cancer Biol.*, 2015, **35**, 244.

2 H. Sung, J. Ferlay, R. L. Siegel, M. Laversanne, I. Soerjomataram, A. Jema and F. Bray, *Ca-Cancer J. Clin.*, 2021, **71**, 209–249.

3 L. Y. Ramirez, S. E. Huestis, T. Y. Yap, S. Zyzanski, D. Drotar and E. Kodish, *Pediatr. Blood Cancer*, 2009, **52**, 497.

4 V. Dilalla, G. Chaput, T. Williams and K. Sultanem, *Curr. Oncol.*, 2020, **27**, 107.

5 S. Tan, D. Li and X. Zhu, *Biomed. Pharmacother.*, 2020, **124**, 109821.

6 G. A. R. Gonçalves and R. d M. A. Paiva, *Einstein*, 2017, **1**, 369–375.

7 X. Li, J. F. Lovell, J. Yoon and X. Chen, *Nat. Rev. Clin. Oncol.*, 2020, **17**, 657.

8 S. Chen, Y. Liu, R. Liang, G. Hong, J. An, X. Peng, W. Zheng and F. Song, *Chin. Chem. Lett.*, 2021, **32**, 3903–3906.

9 S. Jia, H. Yuan and R. Hu, *Biomater. Sci.*, 2022, **10**, 4443–4457.

10 Z. Jiang, C. Zhang, X. Wang, M. Yan, Z. Ling, Y. Chen and Z. Liu, *Angew. Chem., Int. Ed.*, 2021, **60**, 22376–22384.

11 R. Qu, X. Zhen and X. Jiang, *CCS Chem.*, 2022, **4**, 401–419.

12 H. Cui, D. Hu, J. Zhang, G. Gao, C. Zheng, P. Gong, X. Xie, Z. Sheng and L. Cai, *Chin. Chem. Lett.*, 2017, **28**, 1391–1398.

13 K. Li, M. Lu, X. Xi and Y. Huang, *Chin. Chem. Lett.*, 2021, **32**, 1010–1016.

14 J. Wei, X. Chena, X. Wang, J. Li, S. Shi, G. Liu and N. Zheng, *Chin. Chem. Lett.*, 2017, **28**, 1290–1299.

15 Z. Meng, B. Wang, Y. Liu, Y. Wan, Q. Liu, H. Xu, R. Liang, Y. Shi, P. Tu, H. Wu and C. Xu, *Regener. Biomater.*, 2022, **9**, rbac051.

16 P. Xu, R. K. Kankala, Y. Li, S. Wang and A. Chen, *Regen Biomater.*, 2022, **9**, rbac072.

17 E. Itzhaki, E. Hadad, N. Moskovits, S. M. Stemmer and S. Margel, *Pharmaceuticals*, 2021, **14**, 648.

18 T. S. Hauck, R. E. Anderson, H. C. Fischer, S. Newbigging and W. C. Chan, *Small*, 2010, **6**, 138.

19 Z. Wang, X. Wang, J.-B. Wan, F. Xu, N. Zhao and M. Chen, *Small*, 2021, **17**, 2103780.

20 Z. Lei, X. Li, X. Luo, H. He, J. Zheng, X. Qian and Y. Yang, *Angew. Chem., Int. Ed.*, 2017, **56**, 2979.

21 D. Liu, M. Zhang, W. Tian, W. Jiang, Y. Sun, Z. Zhao and B. Z. Tang, *Aggregate*, 2022, **00**, e164.

22 Z. Zhao, W. He and B. Z. Tang, *Acc. Mater. Res.*, 2021, **2**, 1251–1260.

23 K. S. Sharath Kumar, Y. R. Girish, M. Ashrafizadeh, S. Mirzaei, K. P. Rakesh, M. Hossein Gholami, A. Zabolian, K. Hushmandi, G. Orive, F. B. Kadumudi, A. Dolatshahi-Pirouz, V. K. Thakur, A. Zarrabi, P. Makvandi and K. S. Rangappa, *Coord. Chem. Rev.*, 2021, **447**, 214135.

24 J. Dai, X. Wu, S. Ding, X. Lou, F. Xia, S. Wang and Y. Hong, *J. Med. Chem.*, 2020, **63**, 1996–2012.

25 Z. Zhao, H. Zhang, J. W. Y. Lam and B. Z. Tang, *Angew. Chem., Int. Ed.*, 2020, **59**, 9888–9907.

26 Z. Zhao and B. Z. Tang, *Natl. Sci. Rev.*, 2021, **8**, nwab079.

27 Z. Zhao, X. Zheng, L. Du, Y. Xiong, W. He, X. Gao, C. Li, Y. Liu, B. Xu, J. Zhang, F. Song, Y. Yu, X. Zhao, Y. Cai, X. He, R. T. K. Kwok, J. W. Y. Lam, X. Huang, D. L. Phillips, H. Wang and B. Z. Tang, *Nat. Commun.*, 2019, **10**, 2952.

28 J. Dai, H. Xue, D. Chen, X. Lou, F. Xi and S. Wang, *Coor. Chem. Rev.*, 2022, **464**, 214552.

29 L. Zitvogel, L. Apetoh, F. Ghiringhelli and G. Kroemer, *Nat. Rev. Immunol.*, 2008, **8**, 59.

30 G. Housman, S. Byler, S. Heerboth, K. Lapinska, M. Longacre, N. Snyder and S. Sarkar, *Cancers*, 2014, **6**, 1769.

31 Z. Xie, T. Fan, J. An, W. Choi, Y. Duo, Y. Ge, B. Zhang, G. Nie, N. Xie, T. Zheng, Y. Chen, H. Zhang and J. S. Kim, *Chem. Soc. Rev.*, 2020, **49**, 8065.

32 C. Xu, R. Ye, H. Shen, J. W. Y. Lam, Z. Zhao and B. Z. Tang, *Angew. Chem., Int. Ed.*, 2022, **61**, e202204604.

33 H. S. Jung, P. Verwilst, A. Sharma, J. Shin, J. L. Sessler and J. S. Kim, *Chem. Soc. Rev.*, 2018, **47**, 2280.

34 H. Ma, X. Yang, J. Ke, C. Wang, L. Peng, F. Hu and H. Yuan, *ACS Biomater. Sci. Eng.*, 2020, **6**, 3217.

35 J. Yu, Y. Ju, L. Zhao, X. Chu, W. Yang, Y. Tian, F. Sheng, J. Lin, F. Liu, Y. Dong and Y. Hou, *ACS Nano*, 2016, **10**, 159.

36 K. Wang, X. Fan, L. Zhao, X. Zhang, X. Zhang, Z. Li, Q. Yuan, Q. Zhang, Z. Huang, W. Xie, Y. Zhang and Y. Wei, *Small*, 2016, **12**, 6568.

This journal is © The Royal Society of Chemistry 2023

J. Mater. Chem. B, 2023, **11**, 5953–5975 | **5973**

37 Y. F. Xiao, F. F. An, J. X. Chen, J. Yu, W. W. Tao, Z. Yu, R. Ting, C. S. Lee and X. H. Zhang, *Small*, 2019, **15**, e1903121.

38 G. Gao, Y.-W. Jiang, W. Sun, Y. Guo, H.-R. Jia, X.-W. Yu, G.-Y. Pan and F.-G. Wu, *Small*, 2019, **15**, 1900501.

39 Y. Guo, X.-Y. Wang, Y.-L. Chen, F.-Q. Liu, M.-X. Tan, M. Ao, J.-H. Yu, H.-T. Ran and Z.-X. Wang, *Acta Biomater.*, 2018, **80**, 308.

40 Y. Chen, H. Li, Y. Deng, H. Sun, X. Ke and T. Ci, *Acta Biomater.*, 2017, **51**, 374.

41 F. Ouyang, X. Zhang, L. Zhang, Y. Liu and Q. Shuai, *J. Photochem. Photobiol. B, Biol.*, 2022, **234**, 112535.

42 K. Ding, L. Wang, J. Zhu, D. He, Y. Huang, W. Zhang, Z. Wang, A. Qin, J. Hou and B. Z. Tang, *ACS Nano*, 2022, **16**, 7535.

43 J. Guo, J. Dai, X. Peng, Q. Wang, S. Wang, X. Lou, F. Xia, Z. Zhao and B. Z. Tang, *ACS Nano*, 2021, **15**, 20042.

44 X. Li, N. Kwon, T. Guo, Z. Liu and J. Yoon, *Angew. Chem.*, 2018, **57**, 11522.

45 Y. Gao, J. Zhang, Z. He, L. Luo and C. Yan, *Org. Electron.*, 2021, **92**, 106105.

46 X. Chen, Y. Li, S. Li, M. Gao, L. Ren and B. Z. Tang, *Adv. Funct. Mater.*, 2018, **28**, 1804362.

47 G. Feng, J. Liu, C. J. Zhang and B. Liu, *ACS Appl. Mater. Interfaces*, 2018, **10**, 11546.

48 F. Hu, Y. Yuan, D. Mao, W. Wu and B. Liu, *Biomaterials*, 2017, **144**, 53.

49 J. Xu, Q. Zheng, X. Cheng, S. Hu, C. Zhang, X. Zhou, P. Sun, W. Wang, Z. Su, T. Zou, Z. Song, Y. Xia, X. Yi and Y. Gao, *J. Nanobiotechnol.*, 2021, **19**, 355.

50 D. Fukumura, J. Kloepper, Z. Amoozgar, D. G. Duda and R. K. Jain, *Nat. Rev. Clin. Oncol.*, 2018, **15**, 325.

51 Q. Hu, Z. Huang, Y. Duan, Z. Fu and L. Bin, *Bioconjugate Chem.*, 2020, **31**, 1268.

52 C. Chen, Z. Wang, S. Jia, Y. Zhang, S. Ji, Z. Zhao, R. T. K. Kwok, J. W. Y. Lam, D. Ding, Y. Shi and B. Z. Tang, *Adv. Sci.*, 2022, **9**, 2104885.

53 J. Mei, Y. Huang and H. Tian, *ACS Appl. Mater. Interfaces*, 2018, **10**, 12217.

54 L. Fu, J. Zhang, C. Wu, W. Wang, D. Wang, Z. Hu and Z. Wang, *Nano Res.*, 2022, **15**, 7286.

55 Z. Wang, L. Yu, Y. Wang, C. Wang, Q. Mu, X. Liu, M. Yu, K. N. Wang, G. Yao and Z. Yu, *Adv. Sci.*, 2022, **9**, 2104793.

56 D. Yan, M. Wang, Q. Wu, N. Niu, M. Li, R. Song, J. Rao, M. Kang, Z. Zhang, F. Zhou, D. Wang and B. Z. Tang, *Angew. Chem., Int. Ed.*, 2022, **61**, 02614.

57 M. Zha, G. Yang, Y. Li, C. Zhang, B. Li and K. Li, *Adv. Healthcare Mater.*, 2021, **10**, 2101066.

58 L. Shen, T. Zhou, Y. Fan, X. Chang, Y. Wang, J. Sun, L. Xing and H. Jiang, *Chin. Chem. Lett.*, 2020, **31**, 1709.

59 J. Dai, M. Wu, Q. Wang, S. Ding, X. Dong, L. Xue, Q. Zhu, J. Zhou, F. Xia, S. Wang and Y. Hong, *Natl. Sci. Rev.*, 2021, **8**, nwab039.

60 R. Noy and J. W. Pollard, *Immunity*, 2014, **41**, 49.

61 X. Gao, D. Mao, X. Zuo, F. Hu, J. Cao, P. Zhang, J. Z. Sun, J. Liu, B. Liu and B. Z. Tang, *Anal. Chem.*, 2019, **91**, 6836.

62 G.-H. Nam, Y. Choi, G. B. Kim, S. Kim, S. A. Kim and I.-S. Kim, *Adv. Mater.*, 2020, **32**, 2002440.

63 X. Xu, G. Deng, Z. Sun, Y. Luo, J. Liu, X. Yu, Y. Zhao, P. Gong, G. Liu, P. Zhang, F. Pan, L. Cai and B. Z. Tang, *Adv. Mater.*, 2021, **33**, 2102322.

64 H. Cao, H. Gao, L. Wang, Y. Cheng, X. Wu, X. Shen, H. Wang, Z. Wang, P. Zhan, J. Liu, Z. Li, D. Kong, Y. Shi, D. Ding and Y. Wang, *ACS Nano*, 2022, **16**, 13992.

65 G. Song, L. Cheng, Y. Chao, K. Yang and Z. Liu, *Adv. Mater.*, 2017, **29**, 1700996.

66 N. Ma, Y.-W. Jiang, X. Zhang, H. Wu, J. N. Myers, P. Liu, H. Jin, N. Gu, N. He, F.-G. Wu and Z. Chen, *ACS Appl. Mater. Interfaces*, 2016, **8**, 28480.

67 Y. Chang, L. He, Z. Li, L. Zeng, Z. Song, P. Li, L. Chan, Y. You, X.-F. Yu, P. K. Chu and T. Chen, *ACS Nano*, 2017, **11**, 4848.

68 Q. Li, L. Hang, W. Jiang, J. Dou, L. Xiao, X. Tang, Y. Yao and Y. Wang, *Biomaterials*, 2020, **257**, 120235.

69 X. He, C. Peng, S. Qiang, L. H. Xiong, Z. Zhao, Z. Wang, R. T. K. Kwok, J. W. Y. Lam, N. Ma and B. Z. Tang, *Biomaterials*, 2020, **238**, 119834.

70 L. Xie, X. Ying, X. Li, X. Tan, T. Zhang, X. Zhang, W. Cai, F. An, X. Liu and S. Han, *Mater. Des.*, 2023, **225**, 111456.

71 A. C. Begg, F. A. Stewart and C. Vens, *Nat. Rev. Cancer*, 2011, **11**, 239.

72 C. Y. Yu, H. Xu, S. Ji, R. T. Kwok, J. W. Y. Lam, X. Li, S. Krishnan, D. Ding and B. Z. Tang, *Adv. Mater.*, 2017, **29**, 1606167.

73 Z. Liu, H. Zou, Z. Zhao, P. Zhang, G. G. Shan, R. T. K. Kwok, J. W. Y. Lam, L. Zheng and B. Z. Tang, *ACS Nano*, 2019, **13**, 11283.

74 W. Sun, L. Luo, Y. Feng, Y. Cai, Y. Zhuang, R. J. Xie, X. Chen and H. Chen, *Angew. Chem.*, 2020, **59**, 9914.

75 J. Sun and X. He, *Aggregate*, 2022, **3**, e282.

76 Y. Huang, Q. Chen, H. Lu, J. An, H. Zhu, X. Yan, W. Li and H. Gao, *J. Mater. Chem. B*, 2018, **6**, 6660.

77 D. Trachootham, J. Alexandre and P. Huang, *Nat. Rev. Drug Discovery*, 2009, **8**, 579.

78 G. Jin, G. Feng, W. Qin, B. Z. Tang, B. Liu and K. Li, *Chem. Commun.*, 2016, **52**, 2752.

79 L. Shi, W. Wu, Y. Duan, L. Xu, S. Li, X. Gao and B. Liu, *ACS Nano*, 2021, **15**, 1841.

80 M. Liu, D. Chang and Y. Li, *Acc. Chem. Res.*, 2017, **50**, 2273.

81 X. Wang, J. Dai, X. Wang, Q. Hu, K. Huang, Z. Zhao, X. Lou and F. Xia, *Talanta*, 2019, **202**, 591.

82 Z. Zhou, J. Song, L. Nie and X. Chen, *Chem. Soc. Rev.*, 2016, **45**, 6597.

83 X.-H. Wang, N. Song, W. Hou, C.-Y. Wang, Y. Wang, J. Tang and Y.-W. Yang, *Adv. Mater.*, 2019, **31**, 1903962.

84 X.-Y. Lou and Y.-W. Yang, *Aggregate*, 2020, **1**, 19.

85 N. Song, Z. Zhang, P. Liu, D. Dai, C. Chen, Y. Li, L. Wang, T. Han, Y. W. Yang, D. Wang and B. Z. Tang, *Adv. Funct. Mater.*, 2021, **31**, 2009924.

86 J. Chen, S. Li, Z. Wang, Y. Pan, J. Wei, S. Lu, Q. W. Zhang, L. H. Wang and R. Wang, *Chem. Sci.*, 2021, **12**, 7727.

5974 | *J. Mater. Chem. B*, 2023, **11**, 5953–5975

This journal is © The Royal Society of Chemistry 2023

87 Y. Wang, N. Niu, Y. Huang, S. Song, H. Tan, L. Wang, D. Wang and B. Z. Tang, *Small Methods*, 2022, **6**, 2200393.

88 Z. Wang, B. Liu, Q. Sun, L. Feng, F. He, P. Yang, S. Gai, Z. Quan and J. Lin, *ACS Nano*, 2021, **15**, 12342.

89 M. Lin, Y. Gao, T. J. Diefenbach, J. K. Shen, F. J. Hornicek, Y. I. Park, F. Xu, T. J. Lu, M. Amiji and Z. Duan, *ACS Appl. Mater. Interfaces*, 2017, **9**, 7941.

90 L. Zhao, J. Peng, Q. Huang, C. Li, M. Chen, Y. Sun, Q. Lin, L. Zhu and F. Li, *Adv. Funct. Mater.*, 2014, **24**, 363.

91 W. Fan, B. Yung, P. Huang and X. Chen, *Chem. Rev.*, 2017, **117**, 13566.

92 S. Yan, P. Sun, N. Niu, Z. Zhang, W. Xu, S. Zhao, L. Wang, D. Wang and B. Z. Tang, *ACS Nano*, 2022, **16**, 9785.

93 R. Jiang, J. Dai, X. Dong, Q. Wang, Z. Meng, J. Guo, Y. Yu, S. Wang, F. Xia, Z. Zhao, X. Lou and B. Z. Tang, *Adv. Mater.*, 2021, **33**, 2101158.

94 Z. Lei and F. Zhang, *Angew. Chem., Int. Ed.*, 2021, **60**, 16294.

95 C. Li, G. Chen, Y. Zhang, F. Wu and Q. Wang, *J. Am. Chem. Soc.*, 2020, **142**, 14789.

96 Y. Fang, J. Shang, D. Liu, W. Shi, X. Li and H. Ma, *J. Am. Chem. Soc.*, 2020, **142**, 15271.

97 J. Mu, M. Xiao, Y. Shi, X. Geng, H. Li, Y. Yin and X. Chen, *Angew. Chem., Int. Ed.*, 2022, **61**, 202114722.

98 A. L. Antaris, H. Chen, K. Cheng, Y. Sun, G. Hong, C. Qu, S. Diao, Z. Deng, X. Hu, B. Zhang, X. Zhang, O. K. Yaghi, Z. R. Alamparambil, X. Hong, Z. Cheng and H. Dai, *Nat. Mater.*, 2016, **15**, 235.

99 Y. Qin, X. Chen, Y. Gui, H. Wang, B. Z. Tang and D. Wang, *J. Am. Chem. Soc.*, 2022, **144**, 12825.

100 Y. Li, J. Zhuang, Y. Lu, N. Li, M. Gu, J. Xia, N. Zhao and B. Z. Tang, *ACS Nano*, 2021, **15**, 20453.

This journal is © The Royal Society of Chemistry 2023

J. Mater. Chem. B, 2023, **11**, 5953–5975 | **5975**